Lepton-nucleus scattering within nuclear many-body approaches

Noemi Rocco

UNIVERSITY OF SURREY

‘Nuclear ab initio Theories and Neutrino Physics’ (INT-18-1a)
February 26 - March 30, 2018

Based on:

- NR, A. Lovato, and O. Benhar, Phys. Rev. Lett. **116**, 192501
- NR, A. Lovato, L. Alvarez-Ruso, A. Lovato, and J. Nieves, Phys. Rev. C **96**, 015504 (2017)
- J. E. Sobczyk, NR, A. Lovato, J. Nieves, arXiv:1711.06697
- NR, W. Leidemann, A. Lovato, G. Orlandini, arXiv:1801.07111
- NR, C. Barbieri, arXiv:1803.00825

Motivations

• Atomic nuclei are fascinating many-body systems of strongly interacting fermions.

• In electron- scattering experiments the nucleus is mostly seen as a target, as the kinematic of the probe is completely known.

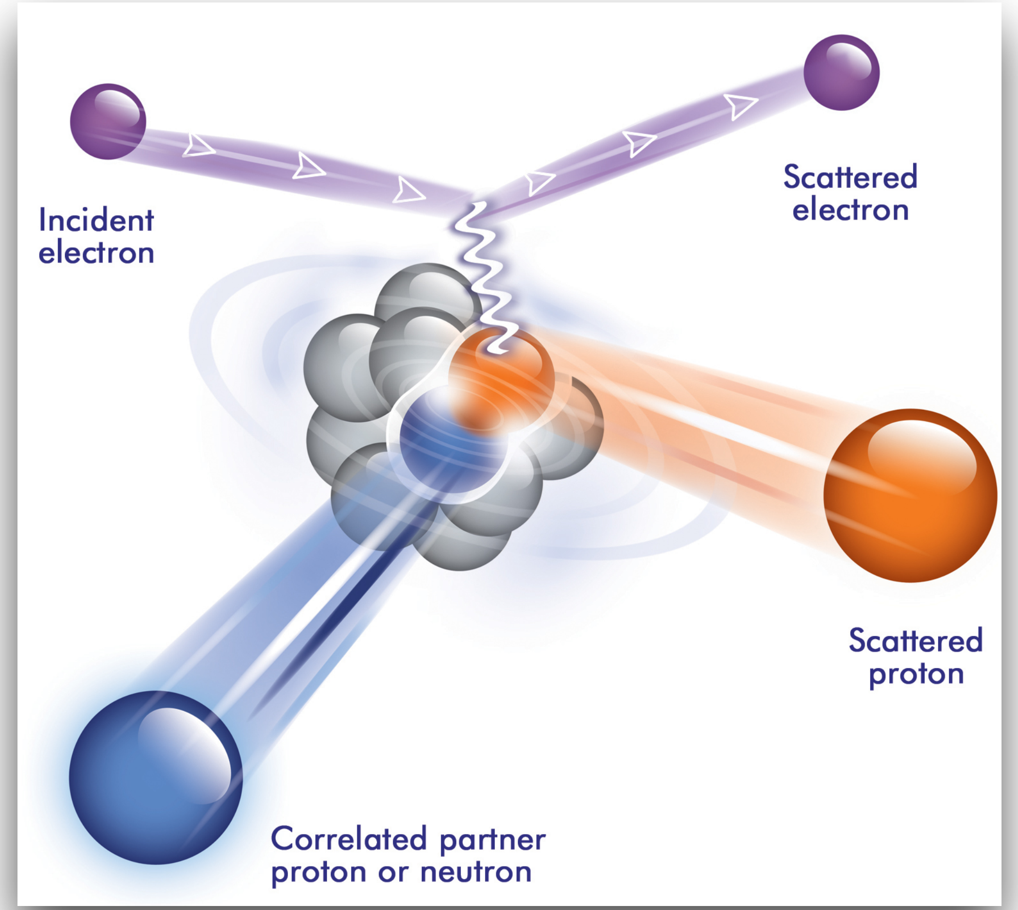

E07-006 : Short Range Correlation Experiment

• This allows to unveil detailed features of the nuclear wave function, including its high-momentum components.

• Developing a coherent picture of the electroweak response is also critical for the interpretation of neutrino scattering experiments, such as the Deep Underground Neutrino Experiment

Motivations

• In neutrino-oscillation experiments the use of nuclear target as detectors allows for a substantial increase of the event rate.

• Understanding neutrino-nucleus interactions in the broad kinematical region relevant to neutrino-oscillation experiments requires an accurate description of both nuclear dynamics and of the interaction vertex

• Oversimplified independent particle model of nuclear structure largely fail to reproduce neutrino scattering data

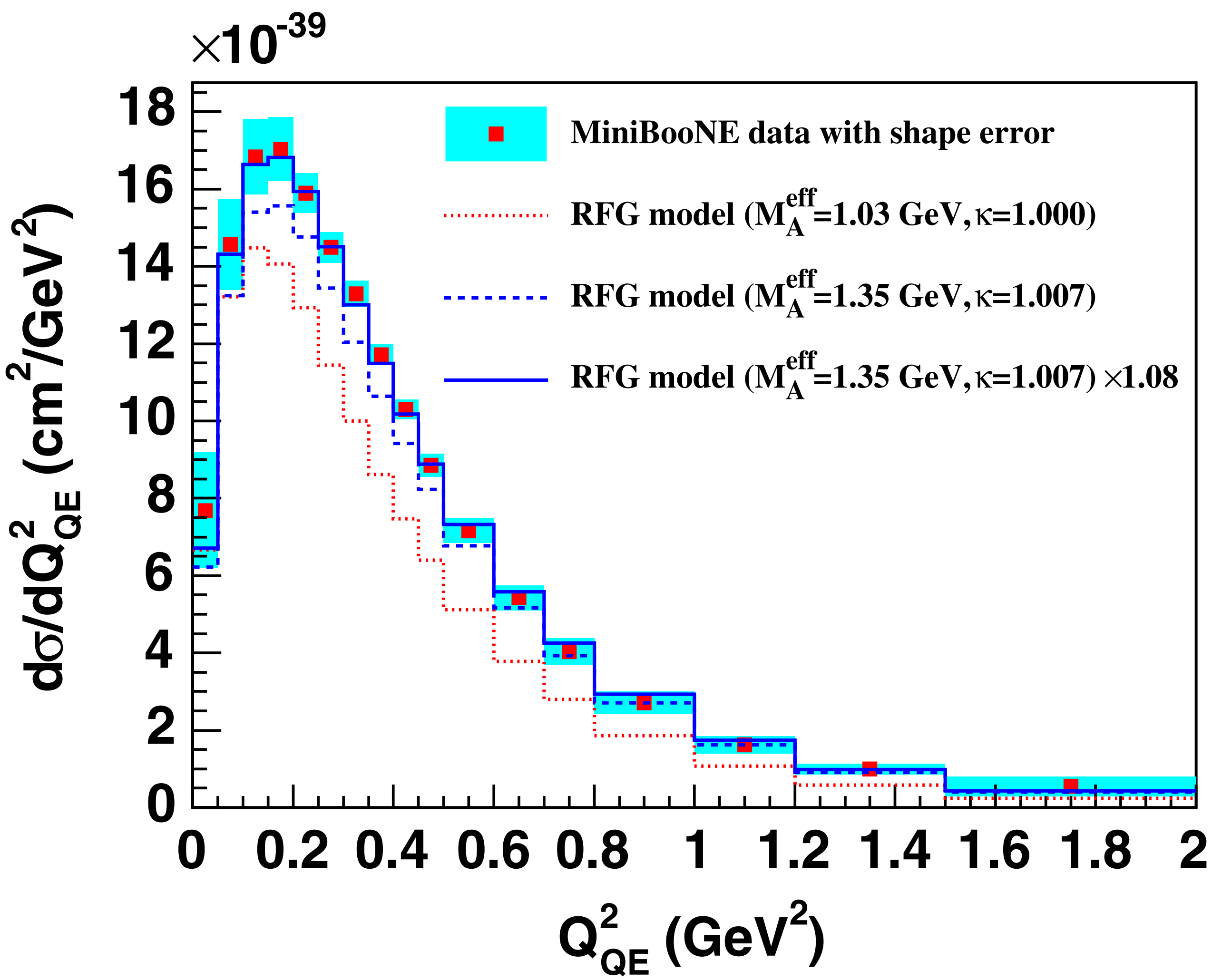

Electron-nucleus scattering

Schematic representation of the inclusive cross section as a function of the energy loss.

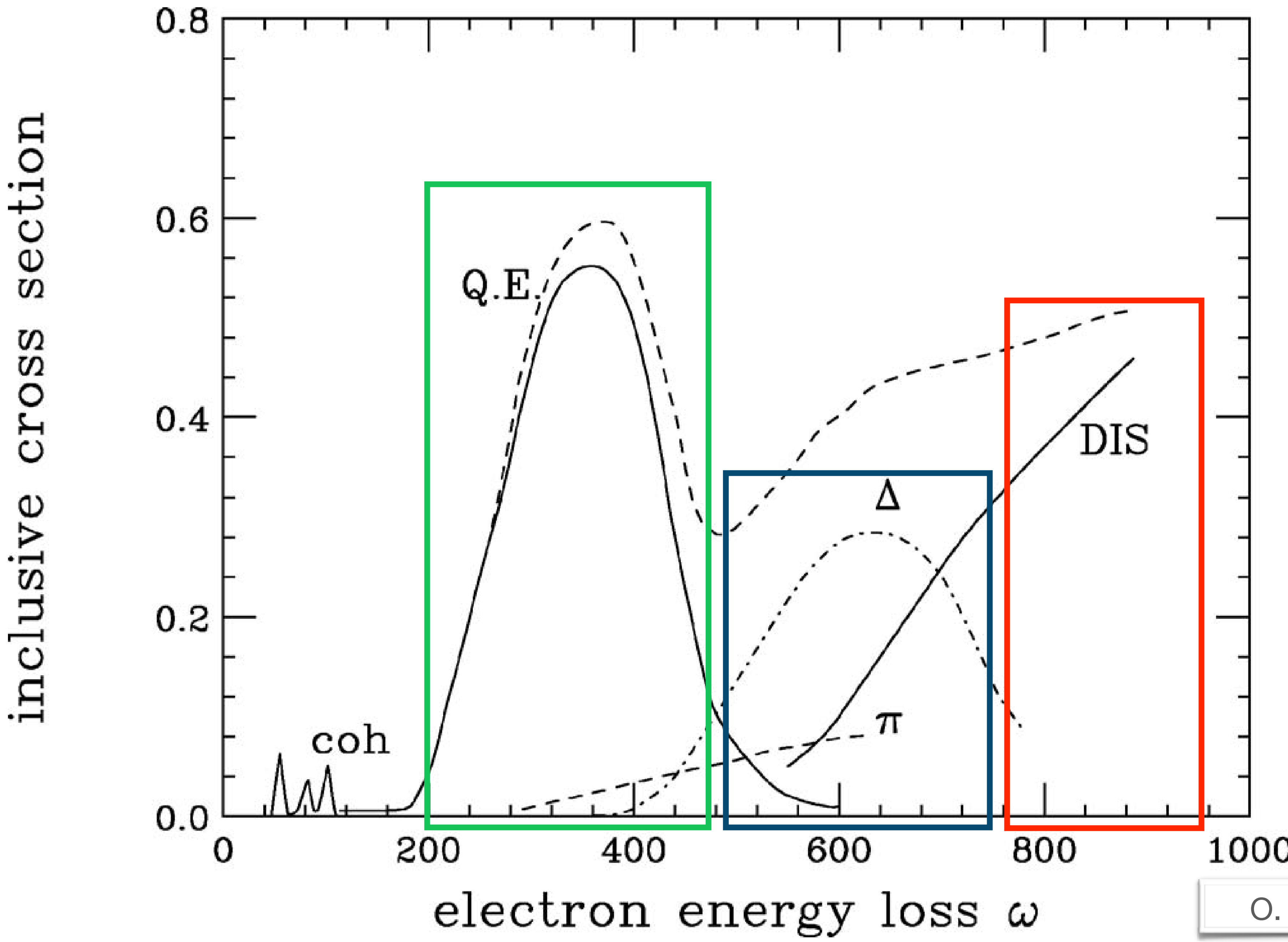

- Broad peak due to quasi-elastic electron-nucleon scattering.
- Excitation of the nucleon to distinct resonances (like the Δ) and pion production.
- Deep Inelastic Scattering region, productions of hadrons other than protons and neutrons

O. Benhar, et al. RMP **80**, 189 (2008)

The different reaction mechanisms can be easily identified

Neutrino-nucleus scattering

The measured double differential CCQE cross section is averaged over the neutrino flux

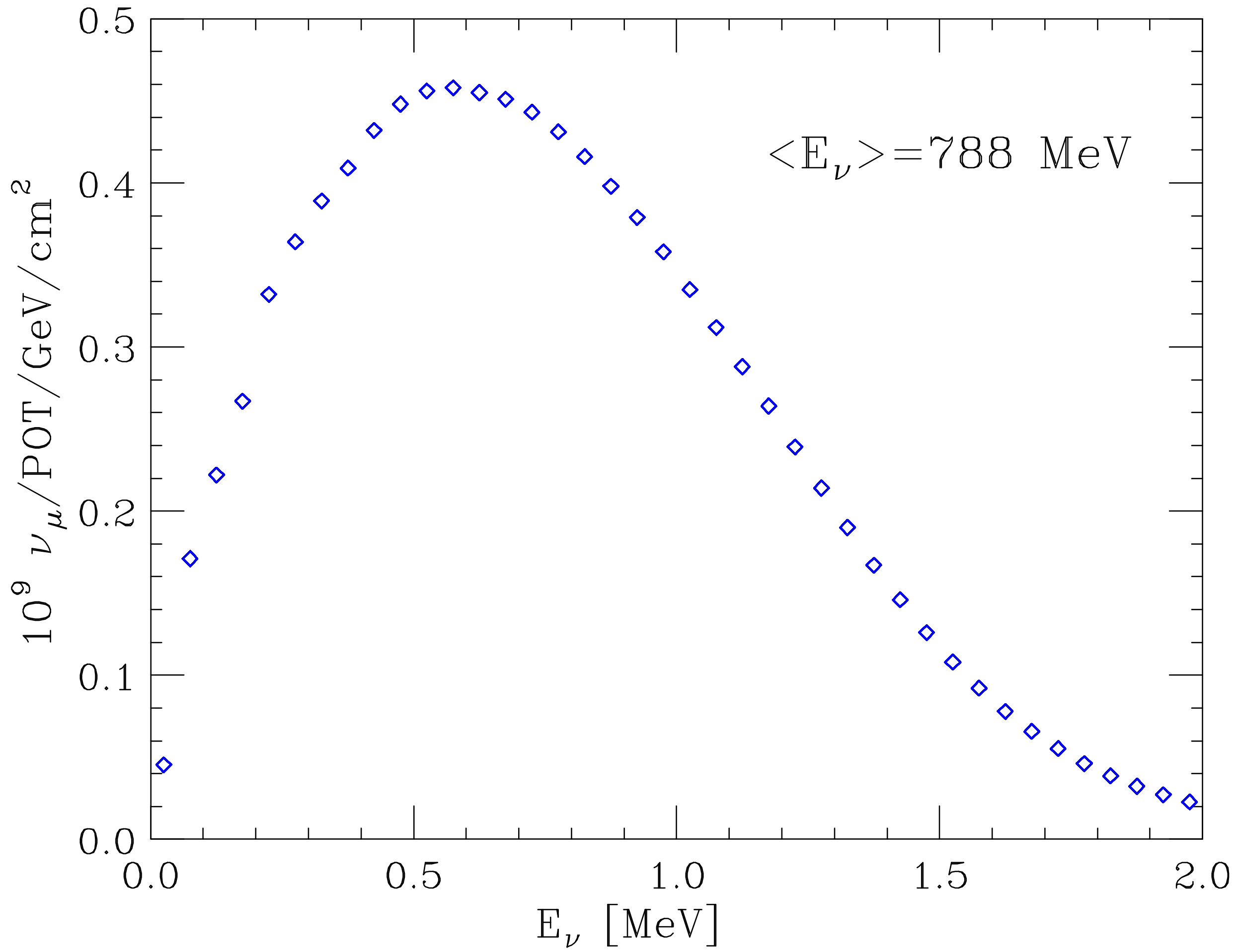

- Energy distribution of the MiniBooNE neutrino flux
- Different reaction mechanisms contribute to the cross section for a fixed value of the kinetic energy and scattering angle of the final lepton
- Processes leading to two-nucleon emission must be taken into account to reproduce the scattering data in the quasi-elastic region

A description of neutrino-nucleus interactions, has to be validated through extensive comparison to the large body of electron-nucleus scattering data.

Electron-nucleus scattering

The inclusive cross section of the process in which a lepton scatters off a nucleus and the hadronic final state is undetected can be written as

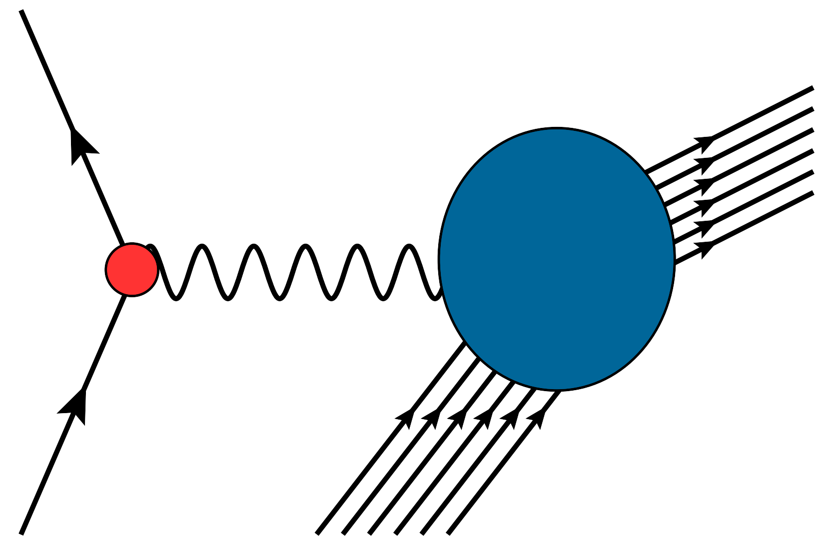

$$\frac{d^2\sigma}{d\Omega_\ell dE_{\ell'}} = L_{\mu\nu} W^{\mu\nu}$$

- The Leptonic tensor is fully specified by the lepton kinematic variables. For instance, in the electron-nucleus scattering case

$$L^{\rm EM}_{\mu\nu} = 2[k_\mu k'_\nu + k_\nu k'_\mu - g_{\mu\nu}(kk')]$$

- The Hadronic tensor contains all the information on target response

$$W^{\mu\nu} = \sum_f \langle 0|J^{\mu\,\dagger}(q)|f\rangle\langle f|J^\nu(q)|0\rangle\delta^{(4)}(p_0 + q - p_f)$$

Non relativistic nuclear many-body theory (NMBT) provides a fully consistent theoretical approach allowing for an accurate description of |0>, independent of momentum transfer.

Non relativistic Nuclear Many Body Theory

• Within the NMBT the nucleus is described as a collection of A point-like nucleons, the dynamics of which are described by the non relativistic Hamiltonian

$$H = \sum_i \frac{\mathbf{p}_i^2}{2m} + \sum_{i<j} v_{ij} + \sum_{i<j<k} V_{ijk} + \dots$$

Argonne v18 (v_{ij}) UIX, IL7 (V_{ijk})

$H\,|0\rangle = E_0\,|0\rangle \quad , \quad H\,|f\rangle = E_f\,|f\rangle$ can be accurately determined for $A \leq 12$

The nuclear electromagnetic current is constrained by the Hamiltonian through the continuity equation

$$\boldsymbol{\nabla} \cdot \mathbf{J}_{\rm EM} + i[H, J^0_{\rm EM}] = 0$$

• The above equation implies that $\mathbf{J}_{\rm EM}$ involves two-nucleon contributions.

• Non relativistic expansion of $\mathbf{J}_{\rm EM}$, powers $|\mathbf{q}|/m$

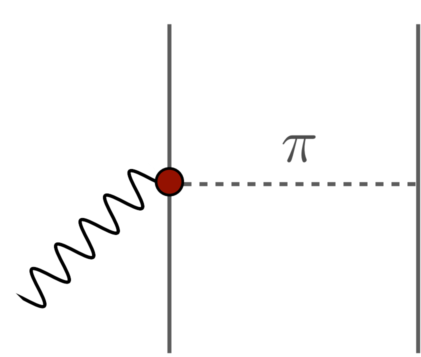

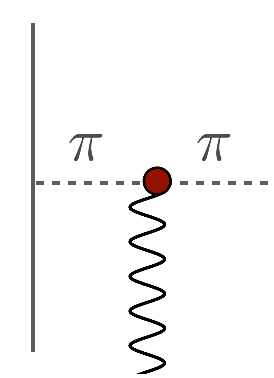

The Green's Function Monte Carlo approach

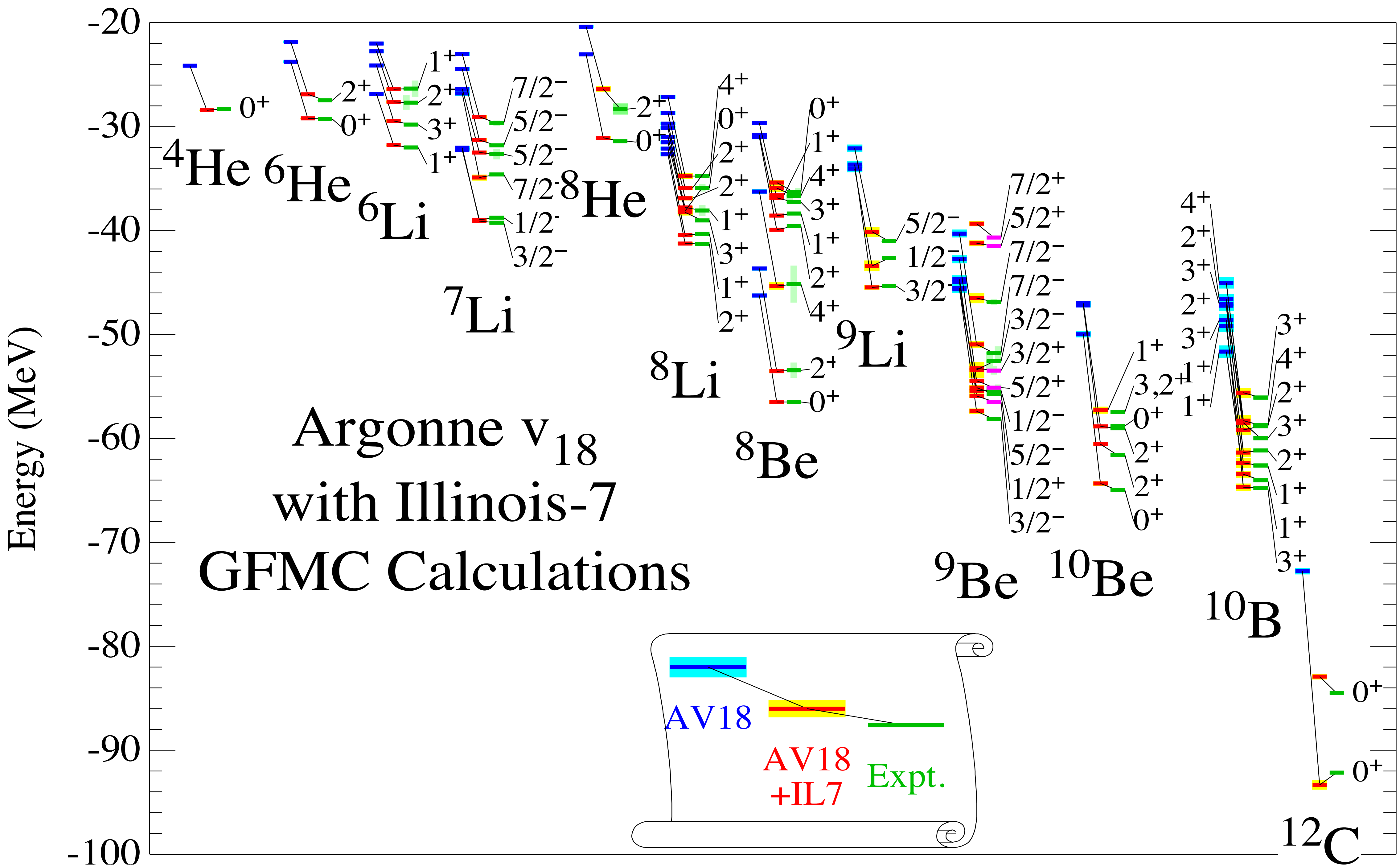

- Green's function Monte Carlo combined with a realistic nuclear hamiltonian reproduces the spectrum of ground and excited states of light nuclei

The Green's Function Monte Carlo approach

• Accurate calculations of the electromagnetic responses of ^{4}He and ^{12}C have been recently performed within GFMC

$$R_{\alpha\beta}(\omega, \mathbf{q}) = \sum_f \langle 0|J_\alpha^\dagger(\mathbf{q})|f\rangle\langle f|J_\beta(\mathbf{q})|0\rangle\delta(\omega - E_f + E_0)$$

• Valuable information on the energy dependence of the response functions can be inferred from the their Laplace transforms

$$E_{\alpha\beta}(\mathbf{q}, \tau) = \int d\omega\, e^{-\omega\tau} R_{\alpha\beta}(\mathbf{q}, \omega) = \langle 0|J_\alpha^\dagger(\mathbf{q})e^{-(H-E_0)\tau}J_\beta(\mathbf{q})|0\rangle$$

Using the completeness relation for the final states, we are left with ground-state expectations value

Limitations of the original method:

★ It is a nonrelativistic method, can not be safely applied in the whole kinematical region relevant for neutrino experiments

★ The computational effort required by the inversion of $E_{\alpha\beta}$ makes the direct calculation of inclusive cross sections unfeasible

Relativistic effects in a correlated system

- We extend the applicability of GFMC in the quasielastic region to intermediate momentum transfers by performing the calculations in a reference frame that minimizes nucleon momenta.
  - The importance of relativity emerges in the frame dependence of non relativistic calculations at high values of **q**
  - In a generic reference frame the longitudinal non relativistic response reads

$$R_L^{fr} = \sum_f \left| \langle\psi_i| \sum_j \rho_j(\mathbf{q}^{fr}, \omega^{fr}) |\psi_f\rangle \right|^2 \delta(E_f^{fr} - E_i^{fr} - \omega^{fr})$$

$$\delta(E_f^{fr} - E_i^{fr} - \omega^{fr}) \approx \delta[e_f^{fr} + (P_f^{fr})^2/(2M_T) - e_i^{fr} - (P_i^{fr})^2/(2M_T) - \omega^{fr}]$$

  - The response in the LAB frame is given by the Lorentz transformation

$$R_L(\mathbf{q}, \omega) = \frac{\mathbf{q}^2}{(\mathbf{q}^{fr})^2} \frac{E_i^{fr}}{M_0} R_L^{fr}(\mathbf{q}^{\mathbf{fr}}, \omega^{fr})$$

where

$$q^{fr} = \gamma(q - \beta\omega),\ \omega^{fr} = \gamma(\omega - \beta q),\ P_i^{fr} = -\beta\gamma M_0,\ E_i^{fr} = \gamma M_0$$

Relativistic effects in a correlated system

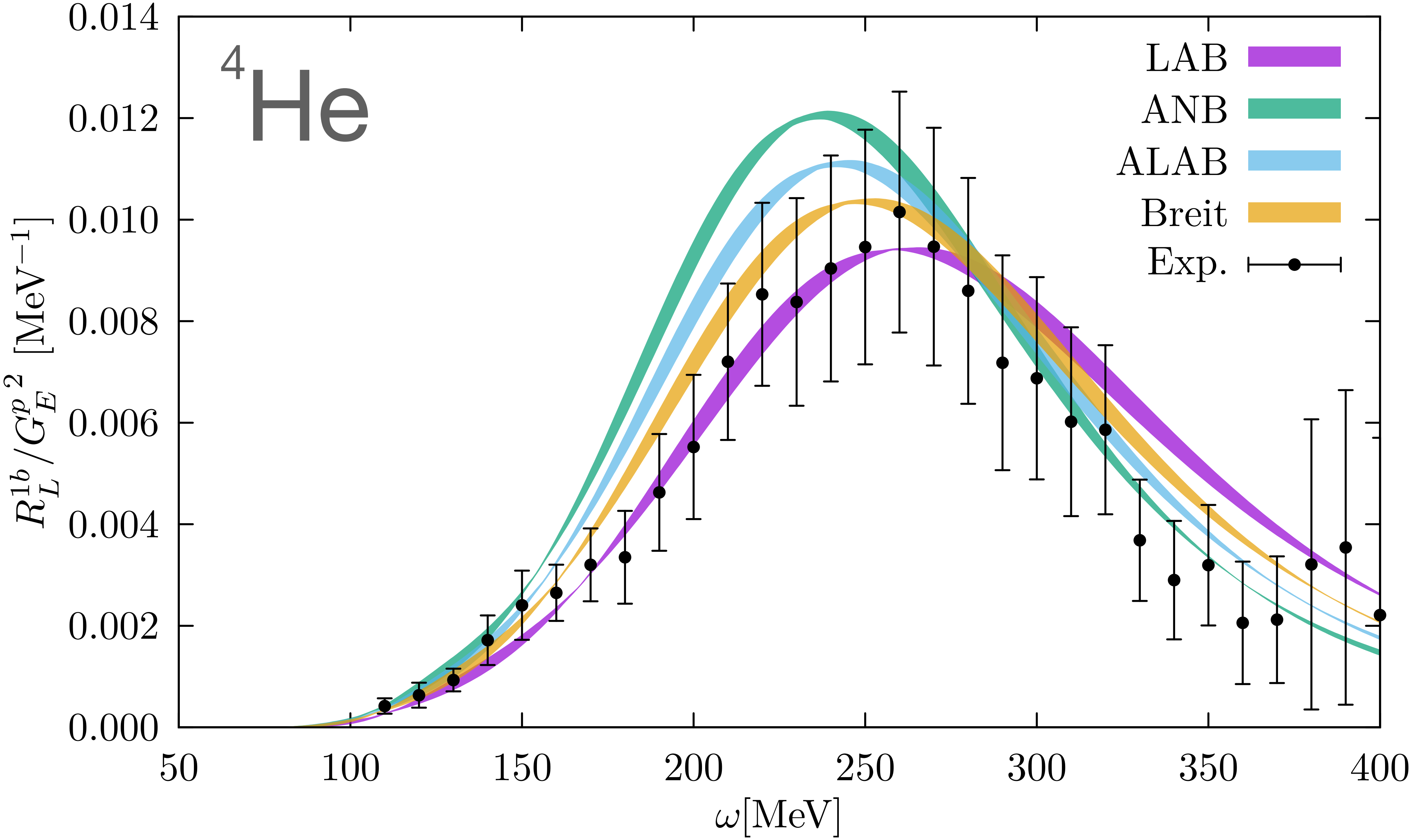

- Longitudinal responses of ^{4}He for |q|=700 MeV in the four different reference frames. The curves show differences in both peak positions and heights.

Relativistic effects in a correlated system

- The frame dependence can be drastically reduced if one assumes a two-body breakup model with relativistic kinematics to determine the input to the non relativistic dynamics calculation

$$p^{fr} = \mu\Big(\frac{p_N^{fr}}{m_N} - \frac{p_X^{fr}}{M_X}\Big)$$
$$P_f^{fr} = p_N^{fr} + p_X^{fr}$$

$$\mu = \frac{m_N M_X}{m_N + M_X}$$

- The relative momentum is derived in a relativistic fashion

$$\omega^{fr} = E_f^{fr} - E_i^{fr}$$
$$E_f^{fr} = \sqrt{m_N^2 + [\mathbf{p}^{fr} + \mu/M_X \mathbf{P}_f^{fr}]^2} + \sqrt{M_X^2 + [\mathbf{p}^{fr} - \mu/m_N \mathbf{P}_f^{fr}]^2}$$

- And it is used as input in the non relativistic kinetic energy

$$e_f^{fr} = (p^{fr})^2/(2\mu)$$

- The energy-conserving delta function reads

$$\delta(E_f^{fr} - E_i^{fr} - \omega^{fr}) = \delta(F(e_f^{fr}) - \omega^{fr}) = \Big(\frac{\partial F^{fr}}{\partial e_f^{fr}}\Big)^{-1} \delta[e_f^{fr} - e_f^{rel}(q^{fr}, \omega^f)]$$

Relativistic effects in a correlated system

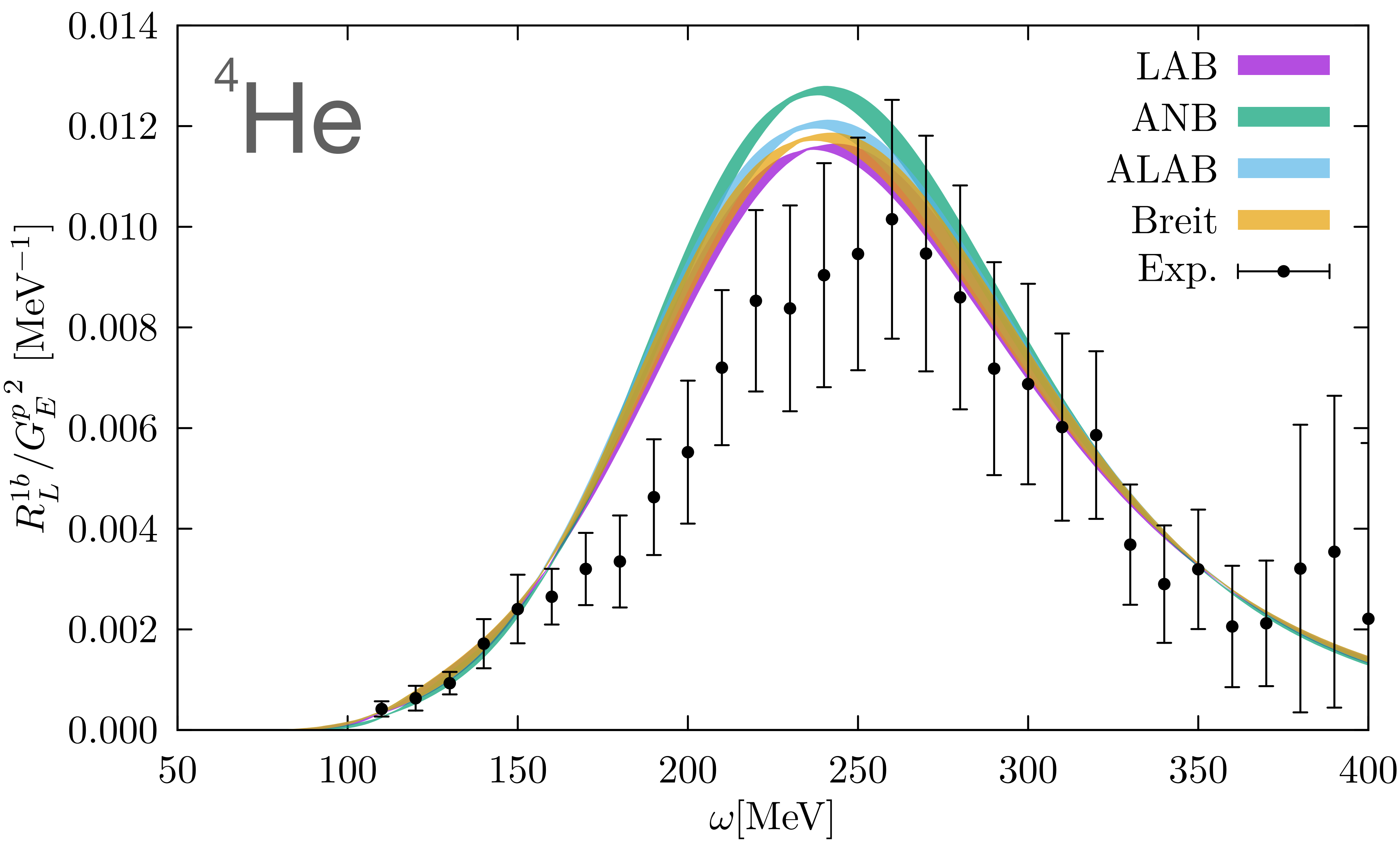

- Longitudinal responses of ^{4}He for |q|=700 MeV in the four different reference frames. The different curves are almost identical.

Scaling in the Fermi gas model

- Scaling of the first kind: the nuclear electromagnetic responses divided by an appropriate function describing the single-nucleon physics no longer depend on the two variables ω and **q**, but only upon $\psi(\mathbf{q}, \omega)$

Adimensional variables:

$$\lambda = \omega/2m$$
$$\kappa = |\mathbf{q}|/2m$$
$$\tau = \kappa^2 - \lambda^2$$
$$\eta_F = p_F/m$$
$$\xi_F = \sqrt{p_F^2 + m^2}/m - 1$$

Scaling function:

$$\psi = \frac{1}{\xi_F} \frac{\lambda - \tau}{\sqrt{(1+\lambda)\tau + \kappa\sqrt{\tau(1+\tau)}}}$$

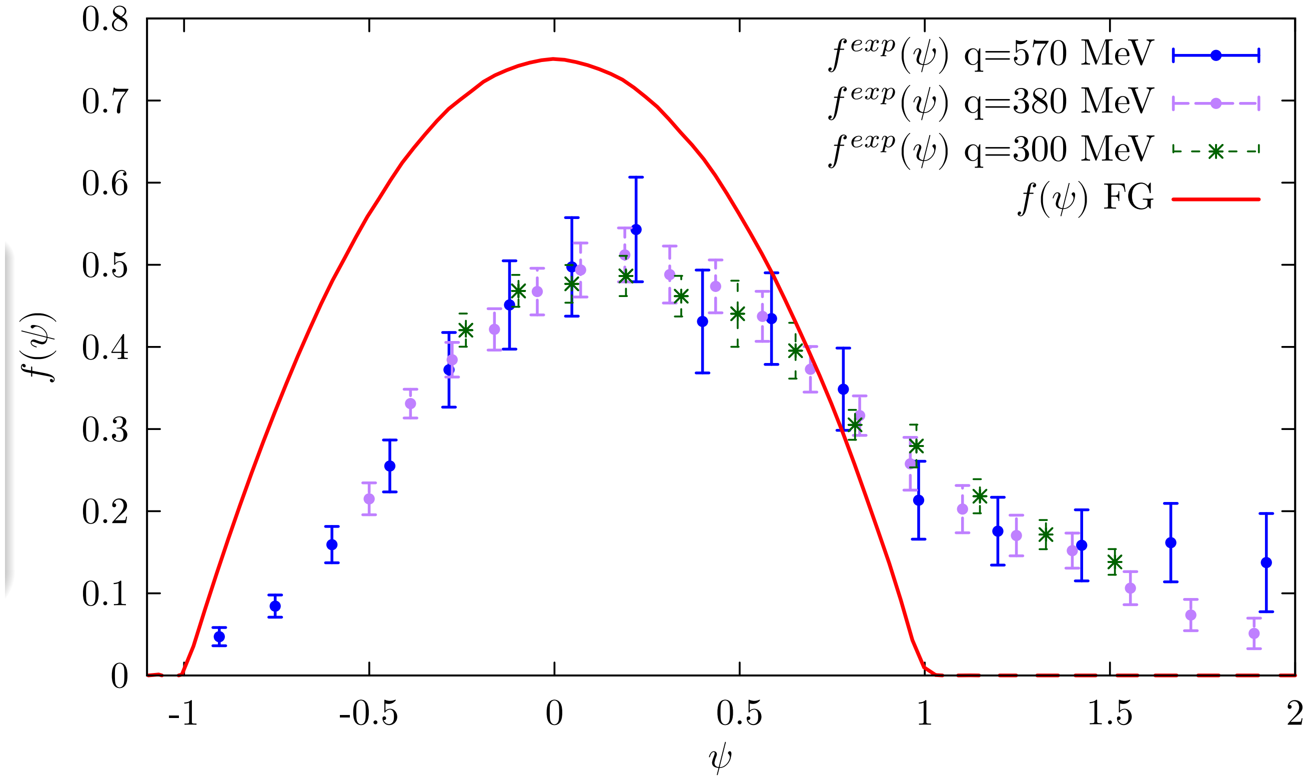

In the FG the L and T responses have the same functional form :

$$R_{L,T} = (1-\psi^2)\theta(1-\psi^2) \times G_{L,T}$$

Scaling as a tool to interpolate the responses

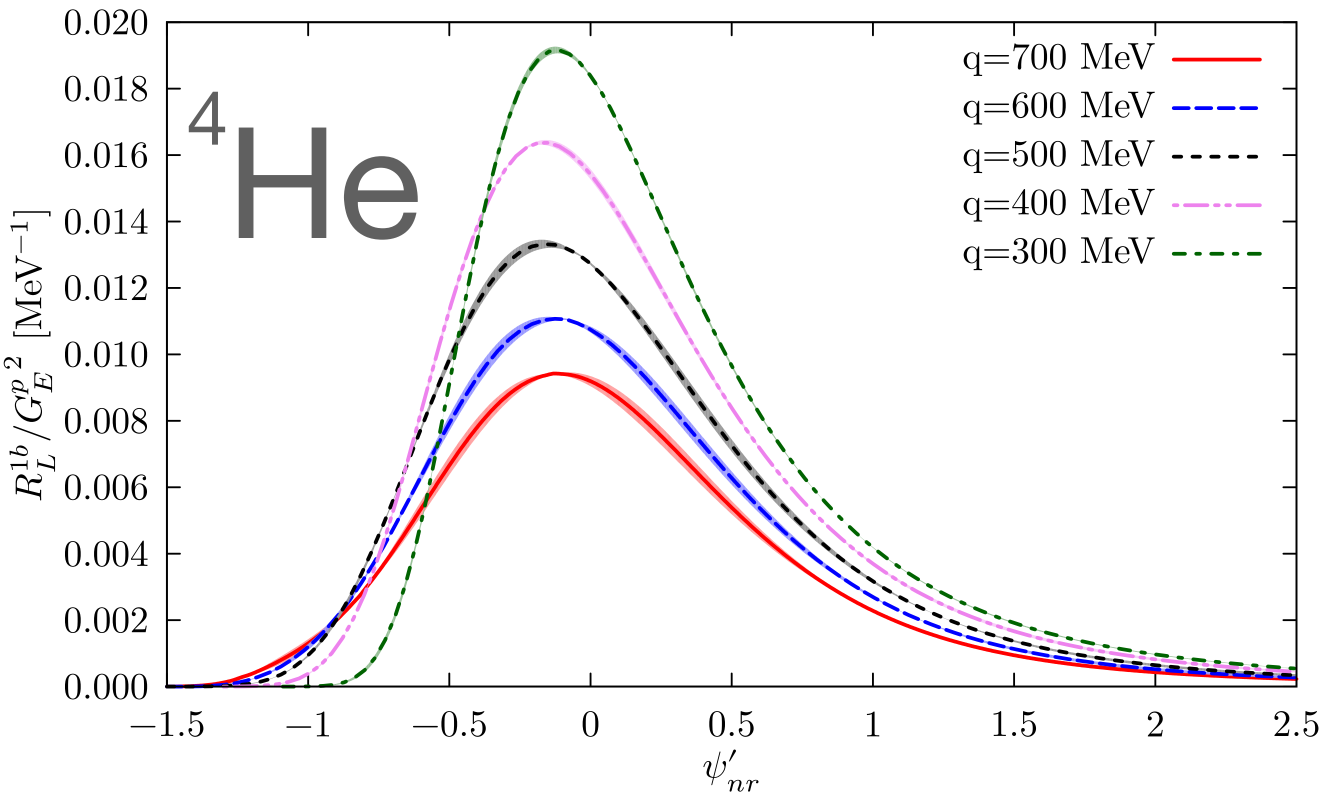

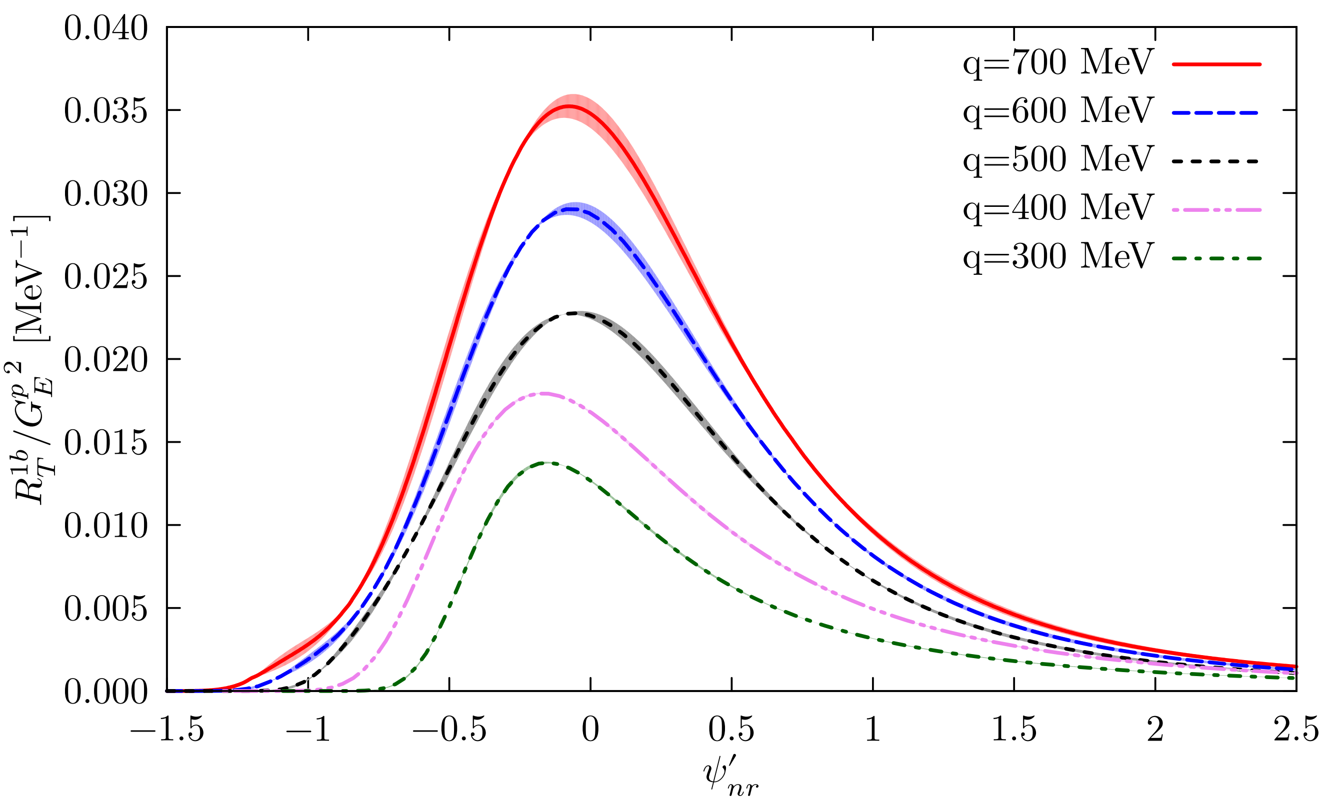

- In order to obtain the GFMC inclusive electron-nucleus cross sections we developed a novel interpolation algorithm based on the scaling of the nuclear responses.

- For a fixed value of E_e and θ_e

$$Q^2 = 4E_e(E_e - \omega)\sin^2\frac{\theta_e}{2}\ ,\ |\mathbf{q}| = \sqrt{Q^2 + \omega^2}$$

- We first compute ψ'_{nr} then the set of $R_{L,T}(\psi'_{nr}, \mathbf{q})$ is interpolated in |**q**|.

- For a given value of ψ'_{nr} the curves corresponding to different values of |**q**| are almost perfectly aligned and monotonic functions of |**q**|. Using the concept of scaling, largely improves the accuracy of the interpolation procedure and reduces the computational cost

Scaling as a tool to interpolate the responses

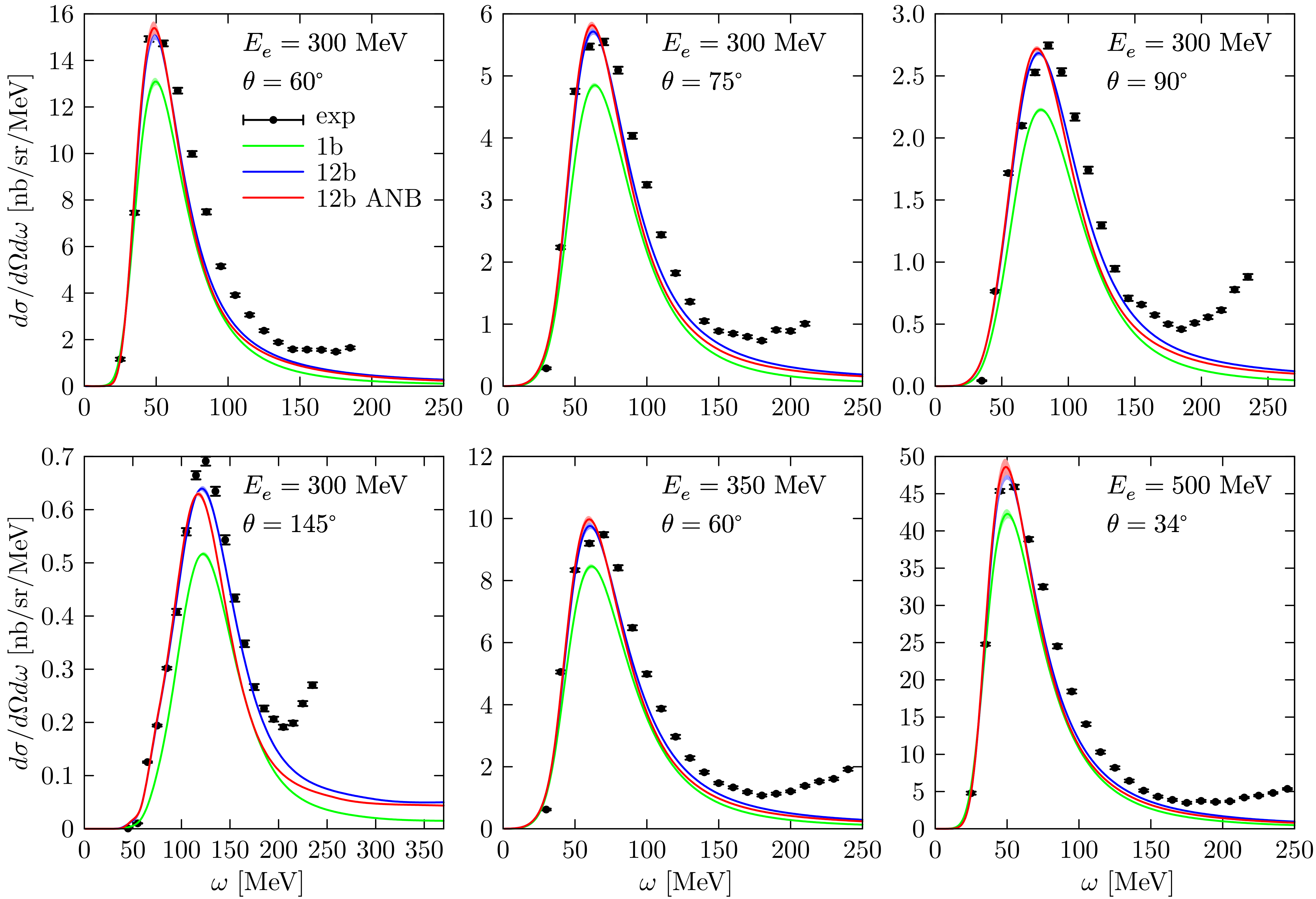

Scaling as a tool to interpolate the responses

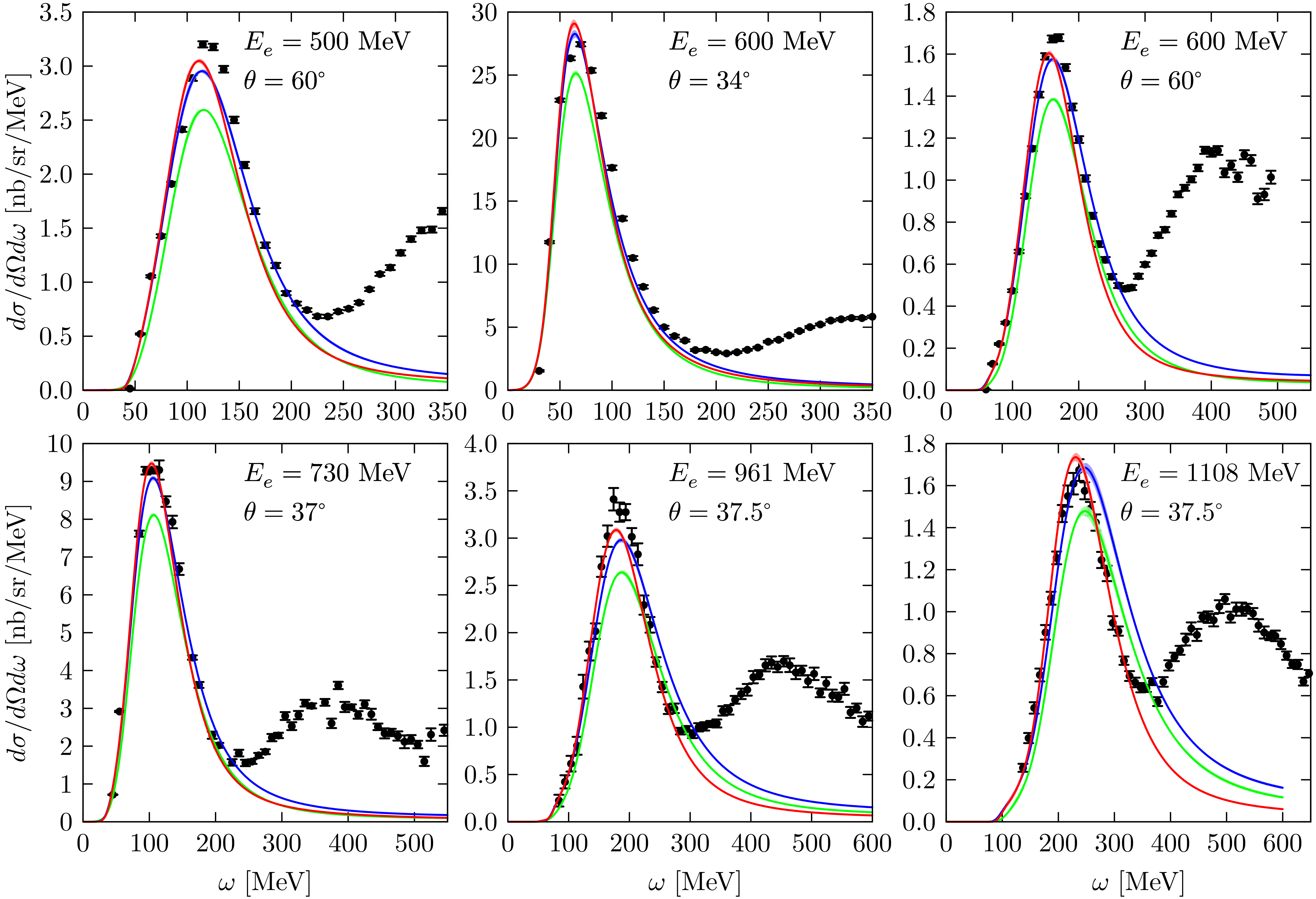

The Impulse Approximation

- For sufficiently large values of |**q**|, the IA can be applied under the assumptions

$$|f\rangle \longrightarrow |p\rangle \otimes |f\rangle_{A-1} \qquad J_\alpha = \sum_i j_\alpha^i$$

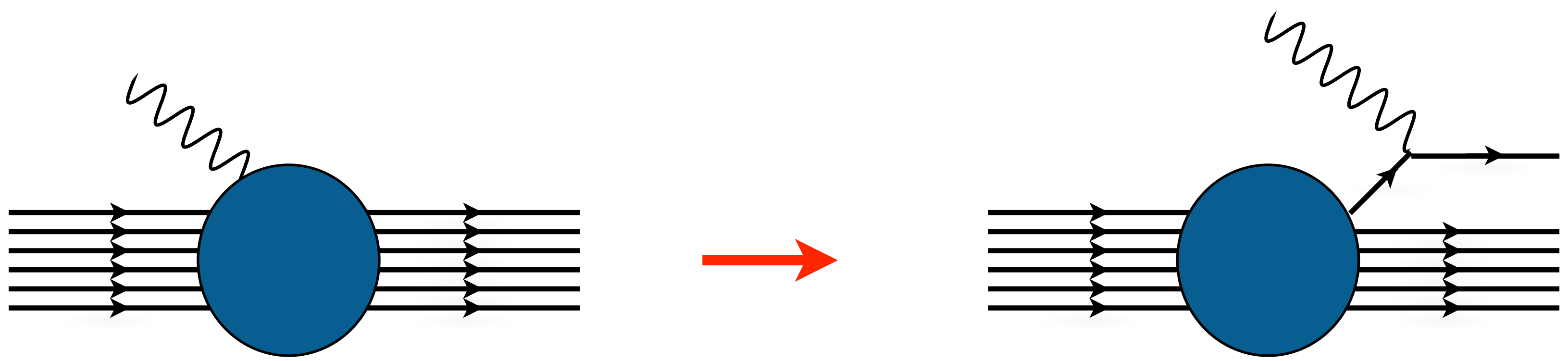

- The matrix element of the current can be written in the factorized form

$$\langle 0|J_\alpha|f\rangle \to \sum_k \langle 0|[|k\rangle \otimes |f\rangle_{A-1}]\langle k|\sum_i j_\alpha^i|p\rangle$$

- The nuclear cross section is given in terms of the one describing the interaction with individual bound nucleons

$$d\sigma_A = \int dE\, d^3k d\sigma_N P(\mathbf{k}, E)$$

- The intrinsic properties of the nucleus are described by the hole spectral function

The one-body hole Spectral Function

- The nuclear matrix element can be rewritten in terms of the transition amplitude

$$[\langle\psi_f^{A-1}|\otimes\langle k|]|\psi_0^A\rangle = \sum_\alpha \mathcal{Y}_{f,\alpha}\tilde{\Phi}_\alpha(\mathbf{k}) = \sum_\alpha \tilde{\Phi}_\alpha(\mathbf{k})\langle\psi_f^{A-1}|a_\alpha|\psi_0^A\rangle\,,$$

- The Spectral Function gives the probability distribution of removing a nucleon with momentum **k**, leaving the spectator system with an excitation energy E

$$P_h(\mathbf{k},E) = \sum_f |\langle\psi_0^A|[|\mathbf{k}\rangle\otimes|\psi_f^{A-1}\rangle]|^2\delta(E+E_f^{A-1}-E_0^A)$$
$$= \frac{1}{\pi}\sum_{\alpha\beta}\tilde{\Phi}^*_\beta(\mathbf{k})\tilde{\Phi}_\alpha(\mathbf{k})\mathrm{Im}\langle\psi_0^A|a_\beta^\dagger\frac{1}{E+(H-E_0^A)-i\epsilon}a_\alpha|\psi_0^A\rangle\,.$$

- The two points Green's Function describes nucleon propagation in the nuclear medium

$$G_{h,\alpha\beta}(E) = \langle\psi_0^A|a_\beta^\dagger\frac{1}{E+(H-E_0^A)-i\epsilon}a_\alpha|\psi_0^A\rangle$$

The Self Consistent Green's Function approach

- The one-body Green's function is completely determined by solving the Dyson equation

$$G_{\alpha\beta}(E) = G^0_{\alpha\beta}(E) + \sum_{\gamma\delta} G^0_{\alpha\gamma} \Sigma^*_{\gamma\delta}(E) G_{\delta\beta}(E)$$

Correlated propagator

initial reference state, HF

Self energy: encoding nuclear medium effects on the particle propagation

- Chiral $NNLO_{sat}$ two and three nucleon forces are used in the calculation

- $\Sigma^* = \Sigma^*[G(E)]$, an iterative procedure is required to solve the Dyson equation self-consistently

- The self-energy is systematically calculated in a non-perturbative fashion within the Algebraic Diagrammatic Construction (ADC).

- Two- and three-nucleon force contributions are included up to the third order → ADC(3)

The Self Consistent Green's Function approach

- To reduce the number of Feynman diagrams entering the calculation of the Green's Function, only interaction irreducible diagrams are considered. The effective one- and two- body interactions are introduced:

$$\tilde{U}_{\alpha\beta} = U_{\alpha\beta} + \sum_{\delta\gamma} V_{\alpha\gamma,\beta\delta}\rho_{\delta\gamma} + \frac{1}{4}\sum_{\mu\nu\gamma\delta} W_{\alpha\mu\nu,\beta\gamma\delta}\rho_{\gamma\mu}\rho_{\nu\delta}\ ,$$

$$\tilde{V}_{\alpha\beta,\delta\gamma} = V_{\alpha\beta,\delta\gamma} + \sum_{\mu\nu} W_{\alpha\beta\mu,\gamma\delta\nu}\rho_{\nu\mu}\ .$$

the one body density matrix reads $\rho_{\delta\gamma} = \langle\psi_0^A|a_\gamma^\dagger a_\delta|\psi_0^A\rangle\ .$

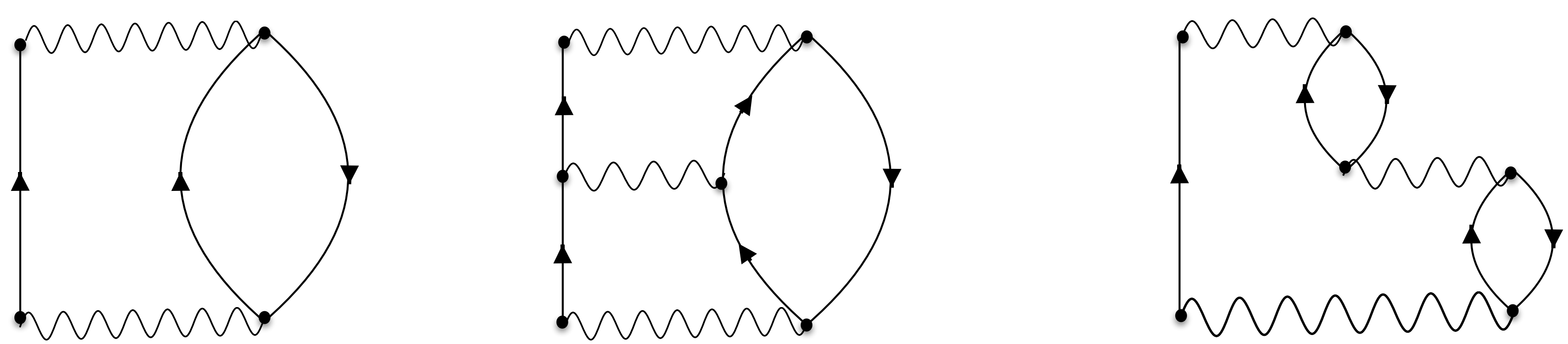

2nd and 3rd order diagrams with 2h1p (and 2p1h) intermediate configurations

- Within the ADC(3) these diagrams are takes as 'seeds' for the infinite order re-summation that eventually generates the self-energy

The Self Consistent Green's Function approach

- Operators are expanded on an harmonic oscillator basis with a given oscillator frequency $\hbar\omega$, and size of the single-particle model space N_{max}

- Point-proton density distribution

$$\rho_p(\mathbf{r}) = \sum_{\alpha\beta} \phi^*_\beta(\mathbf{r})\phi_\alpha(\mathbf{r})\rho_{\alpha\beta}$$

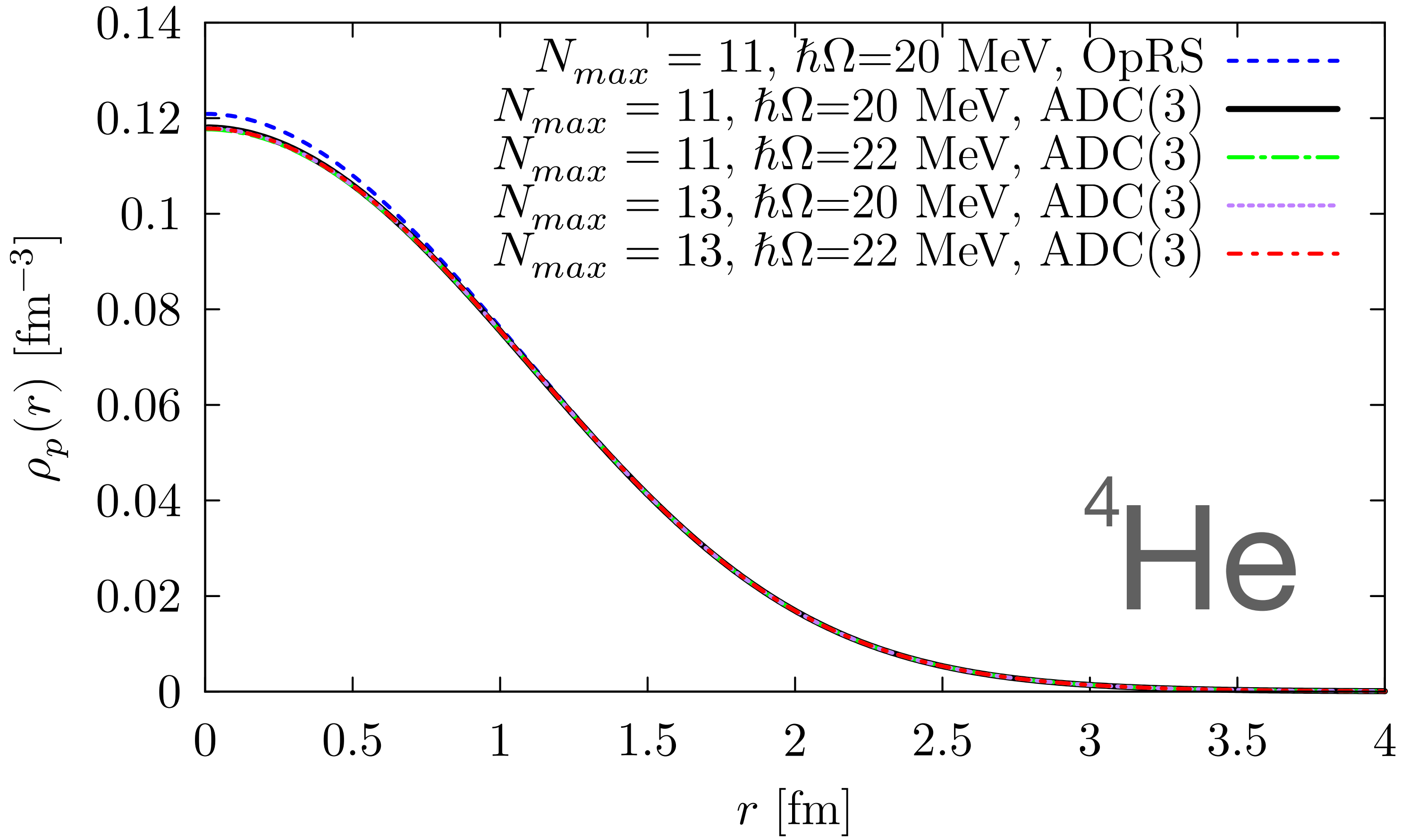

- One-body density matrix

$$\rho_{\alpha\beta} = \langle \Psi_0^A | a^\dagger_\beta a_\alpha | \Psi_0^A \rangle$$

- Optimized Reference State (OpRS) curve is obtained defining an independent particle model propagator:

$$G^{\text{OpRS}}_{\alpha\beta}(E) = + \sum_{k \in F} \frac{\phi^k_\alpha (\phi^k_\beta)^*}{E - \epsilon^{\text{OpRS}}_k - i\eta}$$

where F represents the set of occupied states, ϵ^{OpRS} and ϕ are the single particle energies and wave functions.

- ϵ^{OpRS} and ϕ are obtained by requiring that the OpRS lowest momenta of the spectral distribution reproduce those of the full calculation

The ^{4}He SGFC charge density distribution

- The nuclear charge density distribution is written in terms of the elastic form factor and the Fourier transform of the point proton density distribution

$$\rho_{ch}(r') = \int \frac{d^3q}{(2\pi)^3} e^{-i\mathbf{q}\cdot\mathbf{r}'} \frac{(G_E^p(Q_{el}^2 + G_E^n(Q_{el}^2))\tilde{\rho}_p(q)}{\sqrt{1+Q_{el}^2/(4m^2)}}$$

- The cOm issue: The subtraction of the cOm contribution from the wave function is a long standing problem affecting a number of many-body approaches relying on single nucleon basis

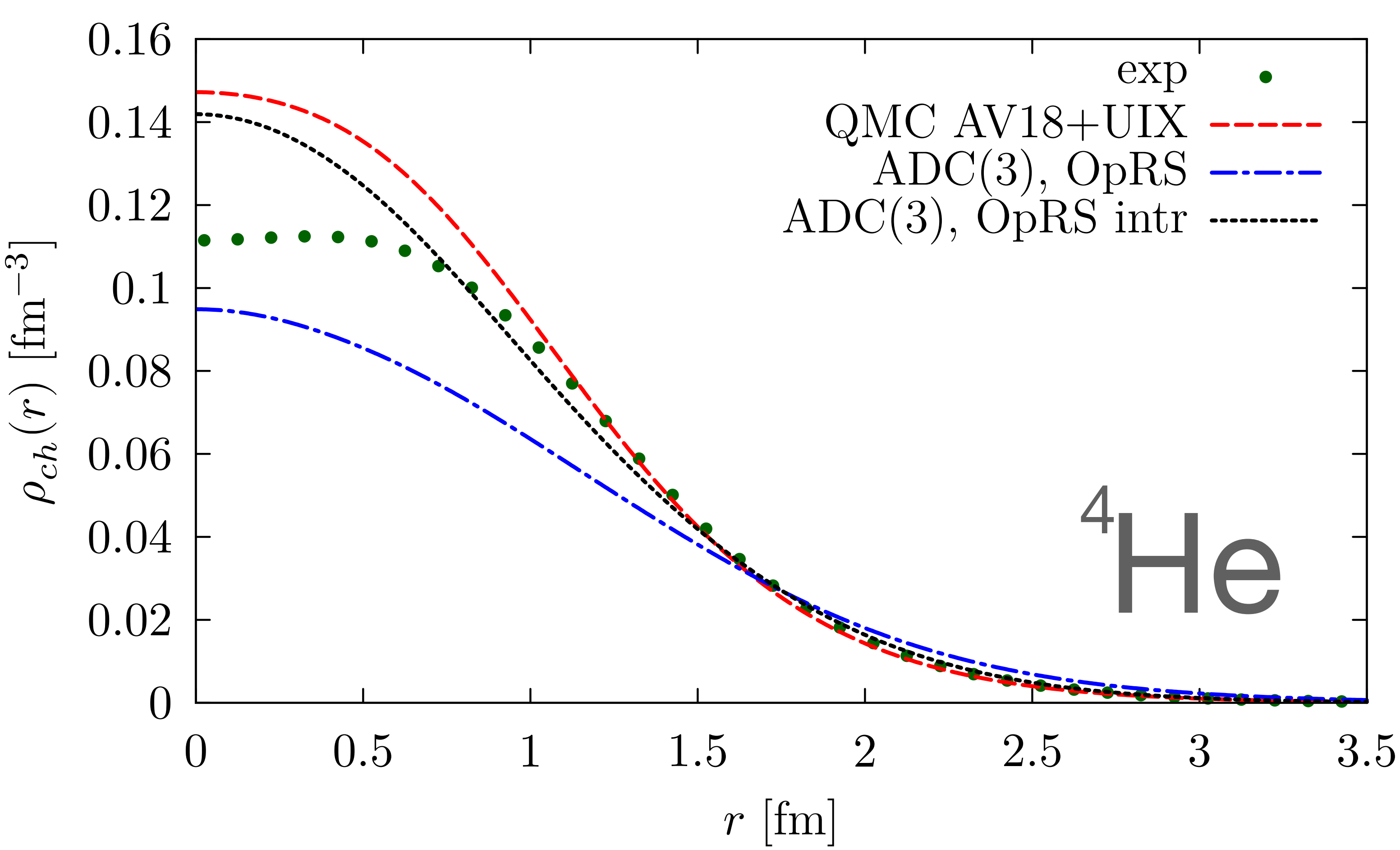

To estimate the error due to residual cOm contribution in ^{4}He we developed Metropolis Monte Carlo calculation

- Trial wave function: $|\psi_V\rangle = |\psi_0^{OpRS}\rangle$
- A sequence of points in the 3A-dimensional space are generated by sampling from $P(\mathbf{R}) = |\psi_0^{OpRS}(\mathbf{R})|^2$
- The intrinsic coordinates are given by

$$\tilde{\mathbf{r}}_i = \mathbf{r}_i - \mathbf{R}_{cm} \ , \ \mathbf{R}_{cm} = \frac{1}{A}\sum_i \mathbf{r}_i$$

The ^{4}He SGFC nucleon momentum distribution

- The nucleon momentum distribution can be defined in terms of the one-body density matrix

$$n(\mathbf{k}) = \sum_{\alpha\beta} \tilde{\phi}^*_\beta(\mathbf{k})\tilde{\phi}_\alpha(\mathbf{k})\rho_{\alpha\beta}$$

- The nucleon momentum distribution is normalized as

$$\int \frac{d^3k}{(2\pi)^3}\, n(\mathbf{k}) = \int \frac{d^3k}{(2\pi)^3}\, dE\, P(\mathbf{k}, E) = A$$

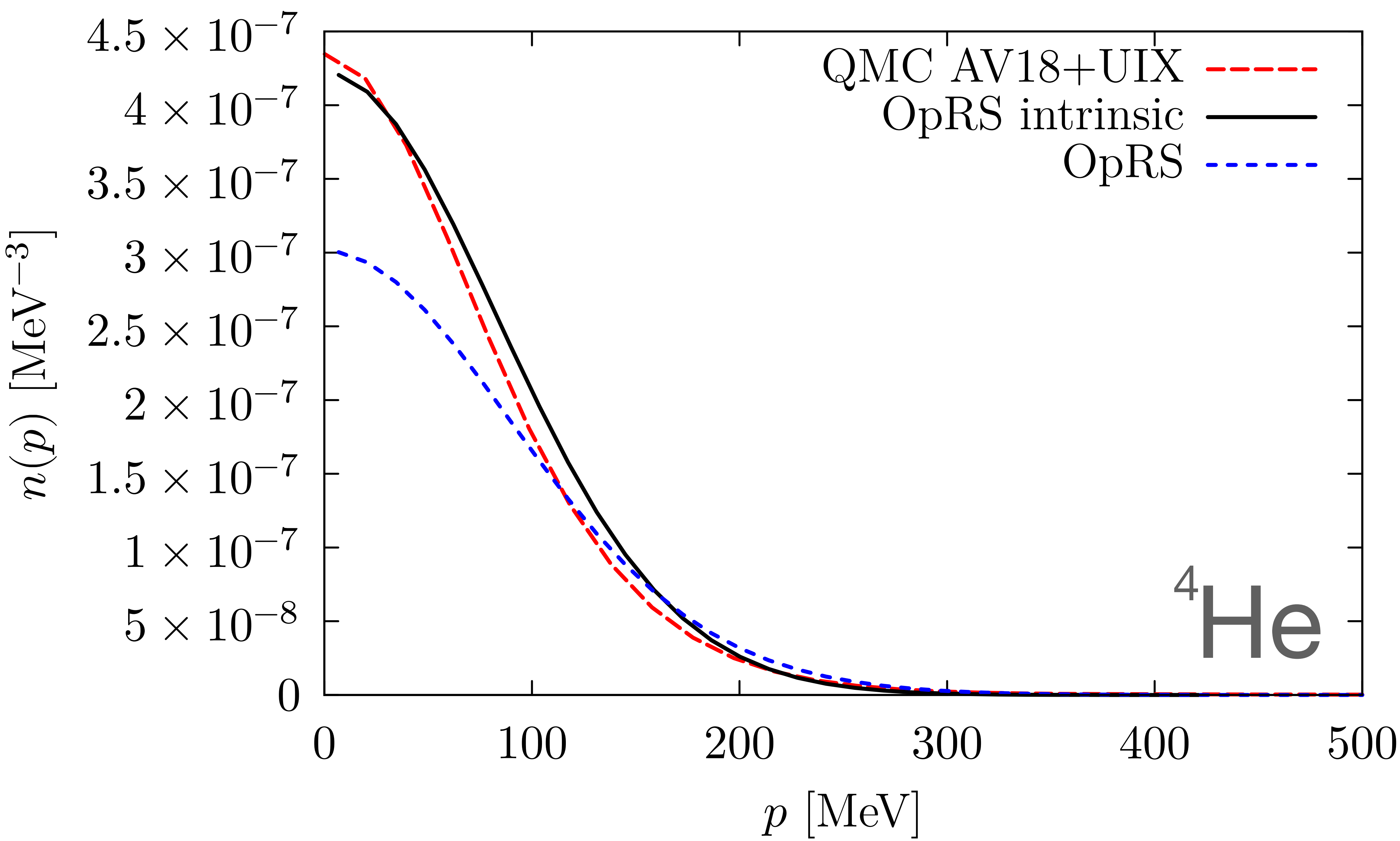

The SGFC results for ^{16}O

- Nuclear charge density distribution of ^{16}O

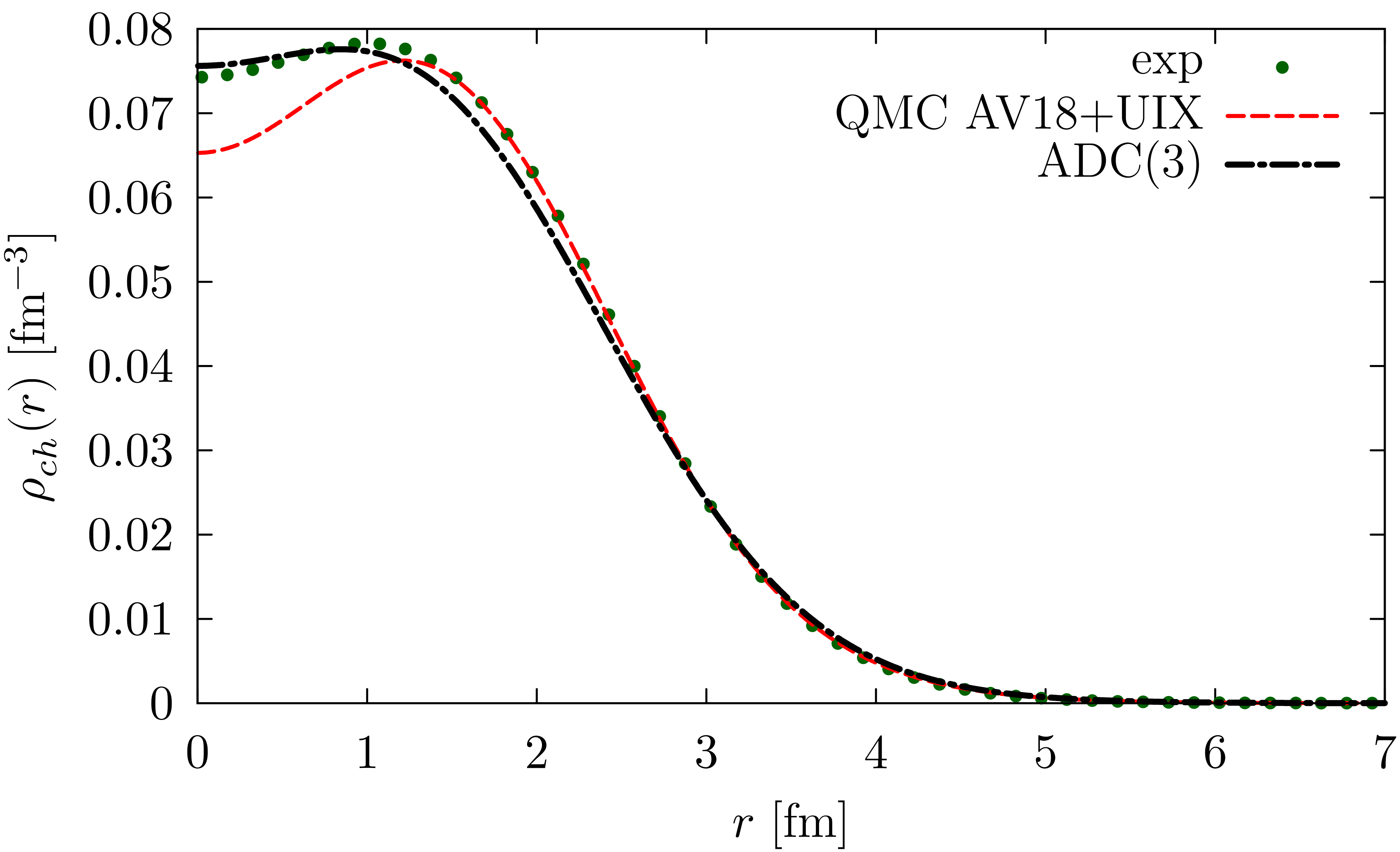

- Nice agreement between the SCGF and QMC calculations

- SCGF results agree with experiments (corroborates the goodness of $NNLO_{sat}$)

The SGFC results for ^{16}O

- Single particle momentum distribution of ^{16}O

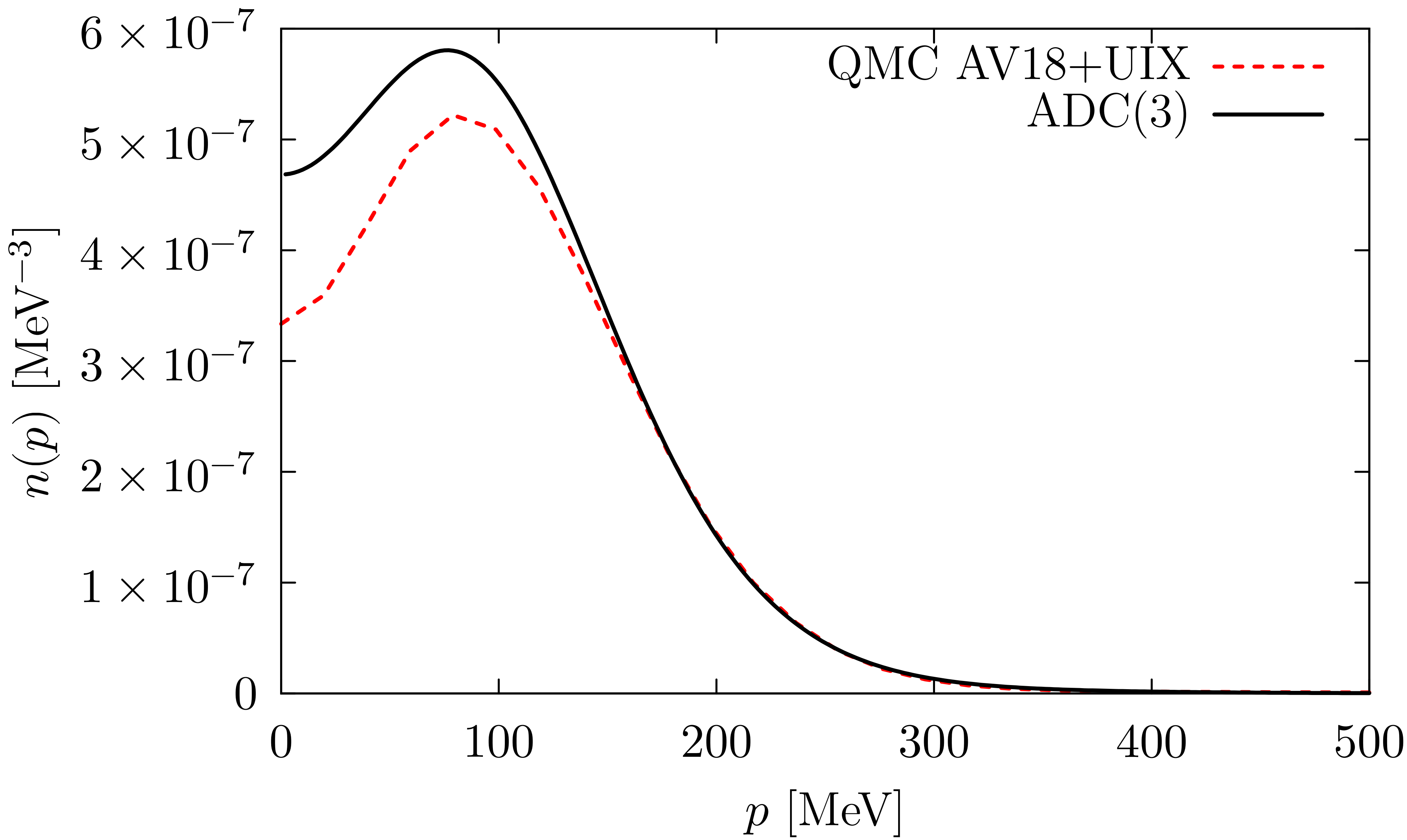

- The momentum distribution reflects the fact that $NNLO_{sat}$ is softer the AV18+UIX.

- QMC accurately treats the high momentum components of the wave function

The SGFC results for ^{16}O

- Single particle momentum distribution of ^{16}O, log scale

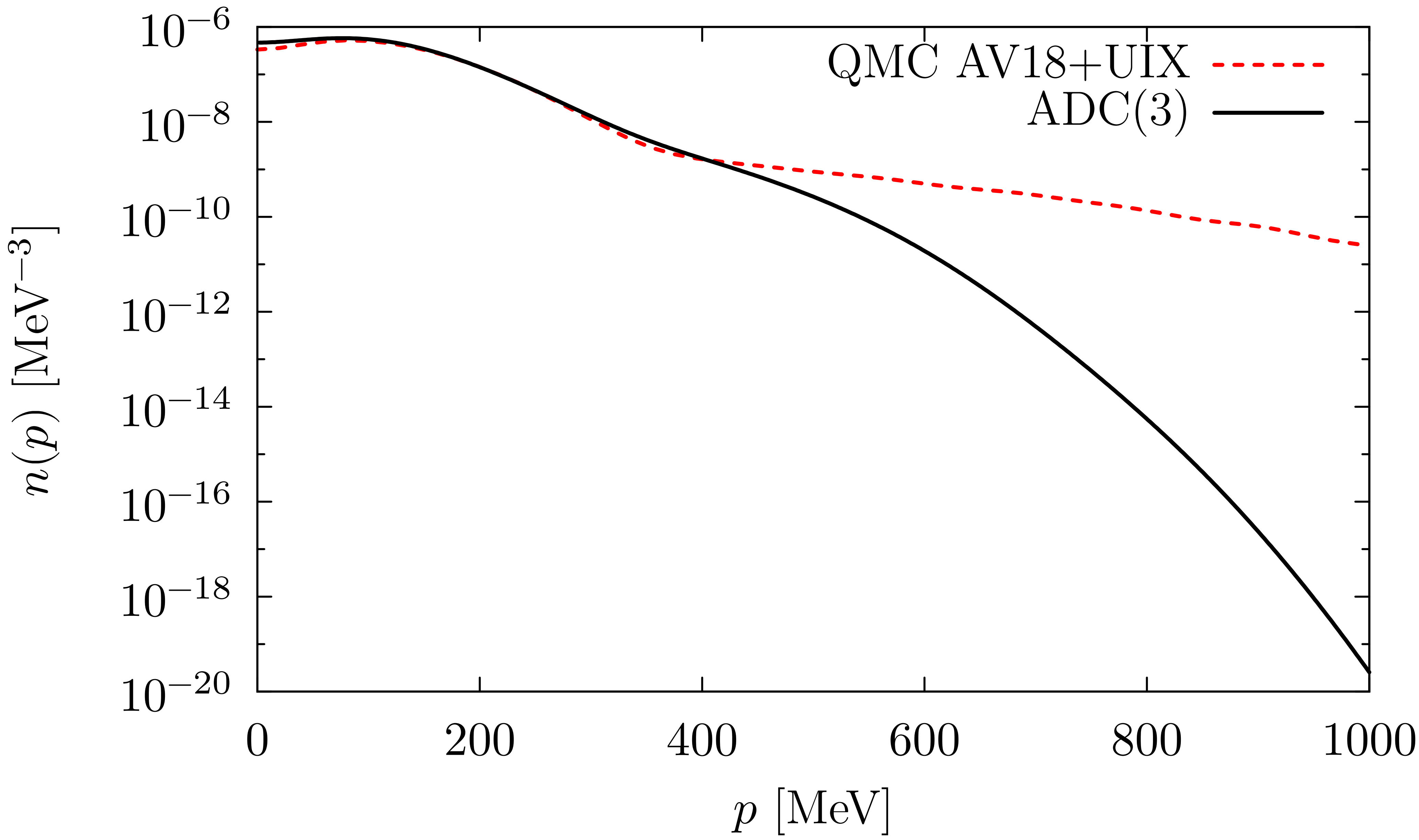

- The momentum distribution reflects the fact that $NNLO_{sat}$ is softer the AV18+UIX.

- QMC accurately treats the high momentum components of the wave function

The Impulse Approximation and convolution scheme

- In the kinematical region in which the interactions between the struck particle and the spectator system can not be neglected, the IA results have to be modified to include the effect of final state interactions (FSI).

$$d\sigma_{FSI} = \int d\omega' f_{\mathbf{q}}(\omega - \omega') d\tilde{\sigma}_{IA} \quad , \quad \tilde{e}(\mathbf{p}) = e(\mathbf{p}) + \mathcal{U}(t_{kin}(\mathbf{p}))$$

Optical Potential

- The theoretical approach to calculate the folding function consists on a generalization of Glauber theory of high energy proton-nucleus scattering

$$f_{\mathbf{q}}(\omega) = \delta(\omega)\sqrt{T_{\mathbf{q}}} + \int \frac{dt}{2\pi} e^{i\omega t} \left[\bar{U}^{FSI}_{\mathbf{q}}(t) - \sqrt{T_{\mathbf{q}}} \right]$$
$$= \delta(\omega)\sqrt{T_{\mathbf{q}}} + (1 - \sqrt{T_{\mathbf{q}}}) F_{\mathbf{q}}(\omega),$$

Glauber Factor

Nuclear Transparency

A.Ankowski et al,Phys. Rev. D91, 033005 (2015)

O.Benhar, Phys. Rev. C87, 024606 (2013)

^{4}He-e$^-$ cross sections within the SCGF approach

- ADC(3) and OpRS results: IA

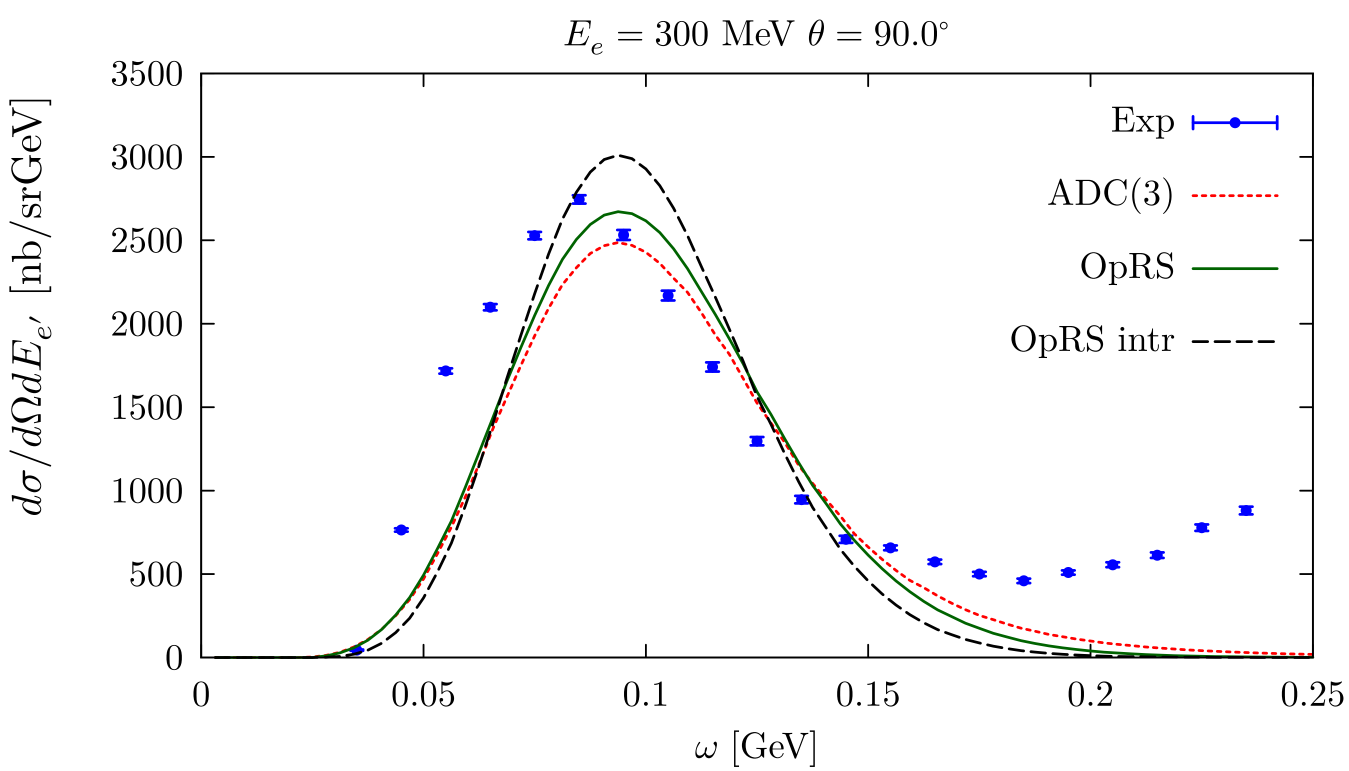

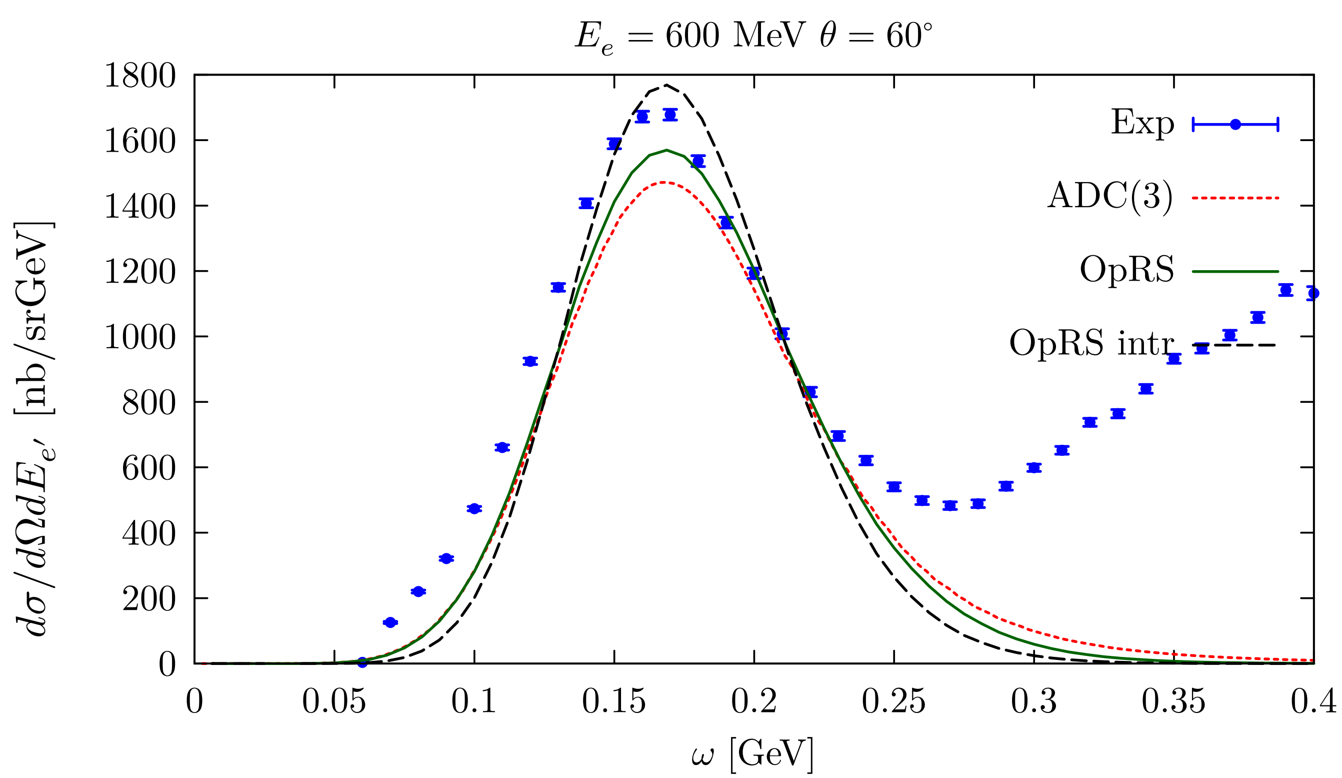

- Including FSI in the OpRS intrinsic results

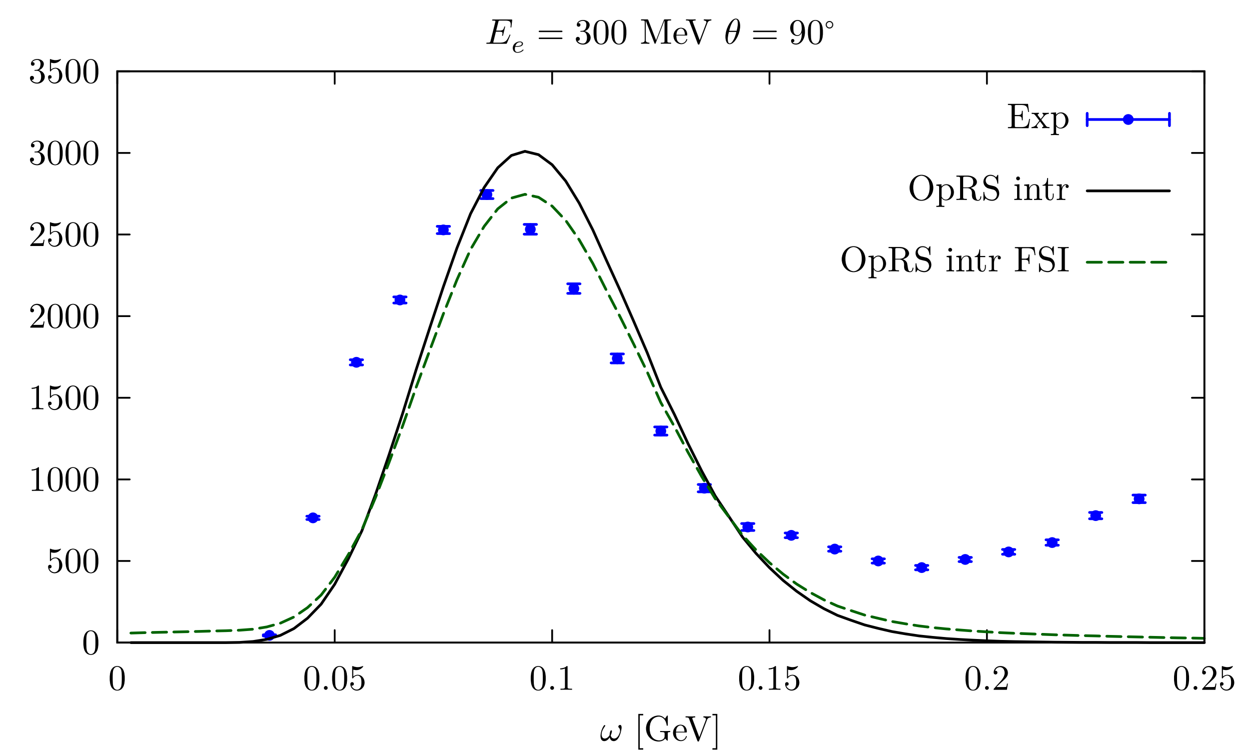

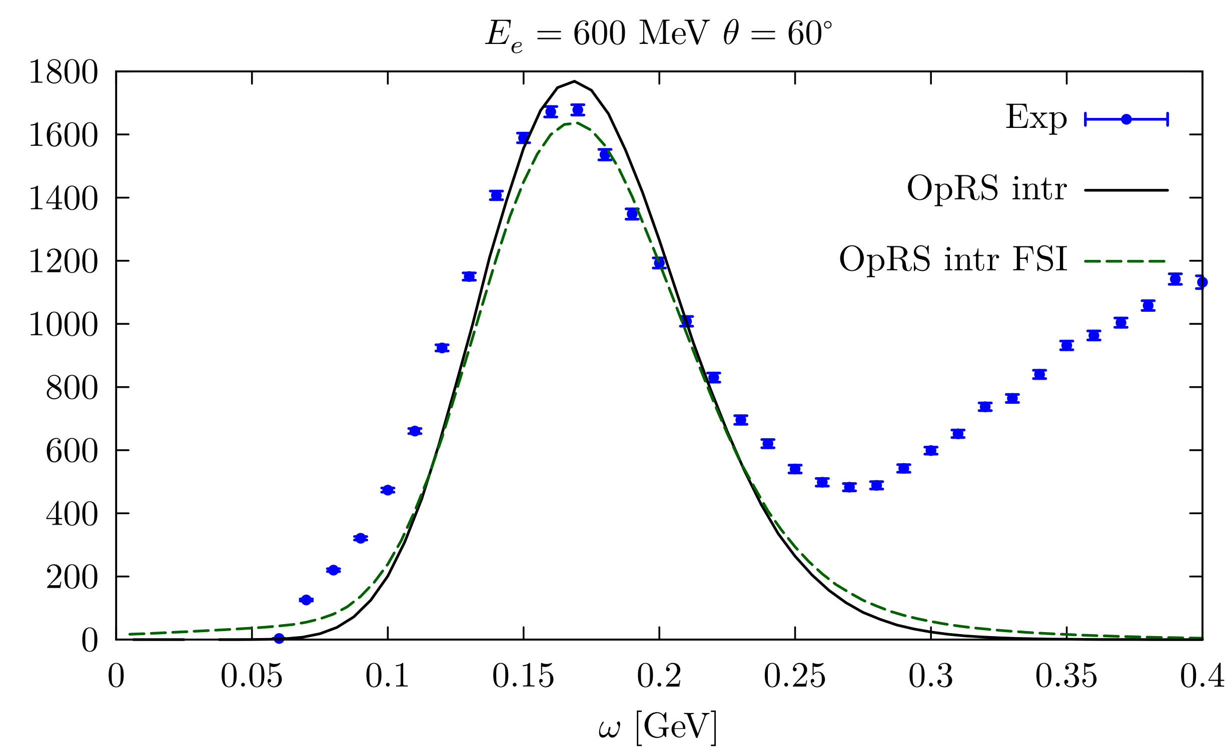

^{16}O-e$^-$ cross sections within the SCGF approach

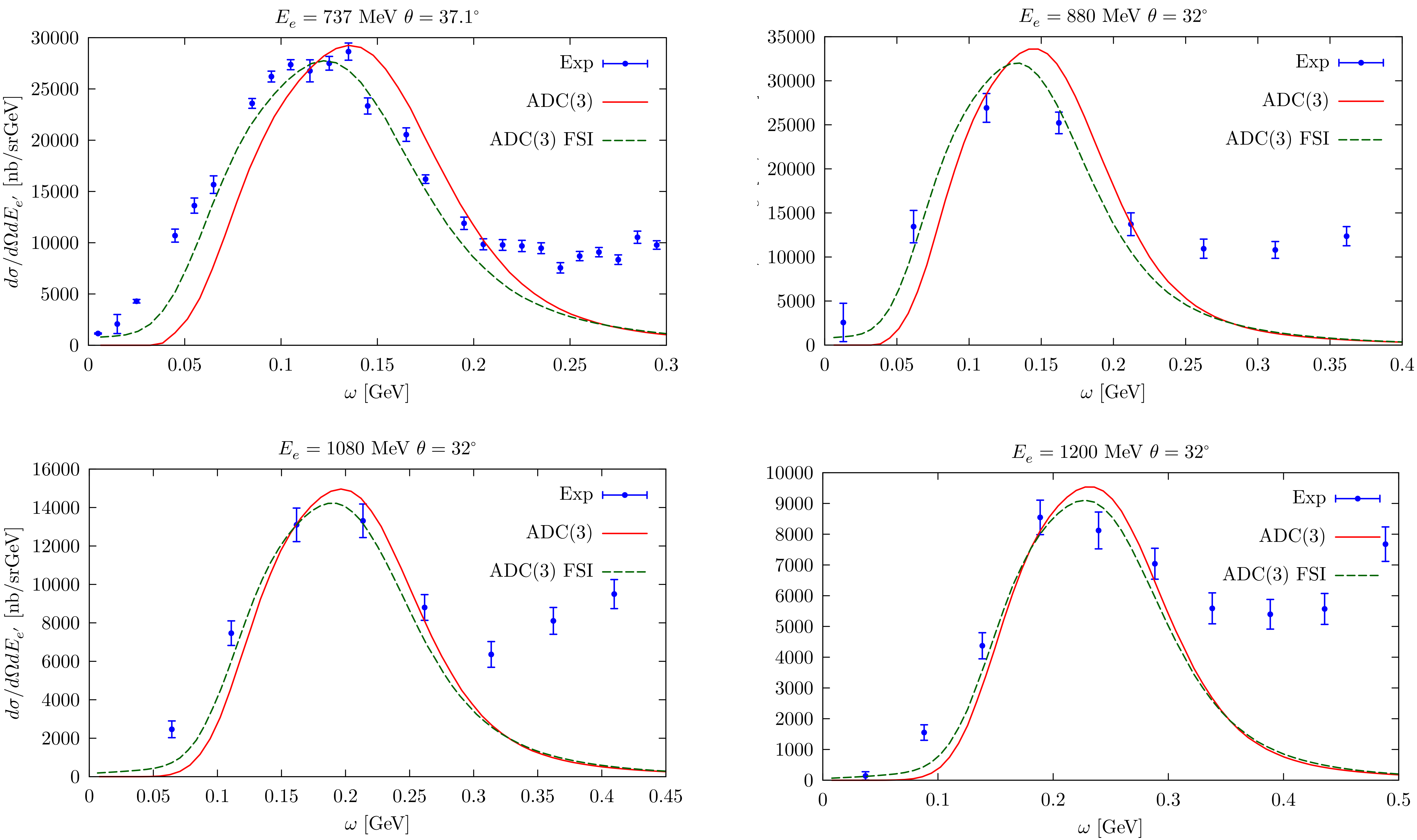

The CBF one-body Spectral Function of finite nuclei

- ^{16}O Spectral Function obtained within CBF and using the Local Density Approximation

$$P_{LDA}(\mathbf{k},E) = P_{MF}(\mathbf{k},E) + P_{corr}(\mathbf{k},E)$$

$$\sum_n Z_n |\phi_n(\mathbf{k})|^2 F_n(E - E_n)$$

^{40}Ar: JLab E 12-14-012

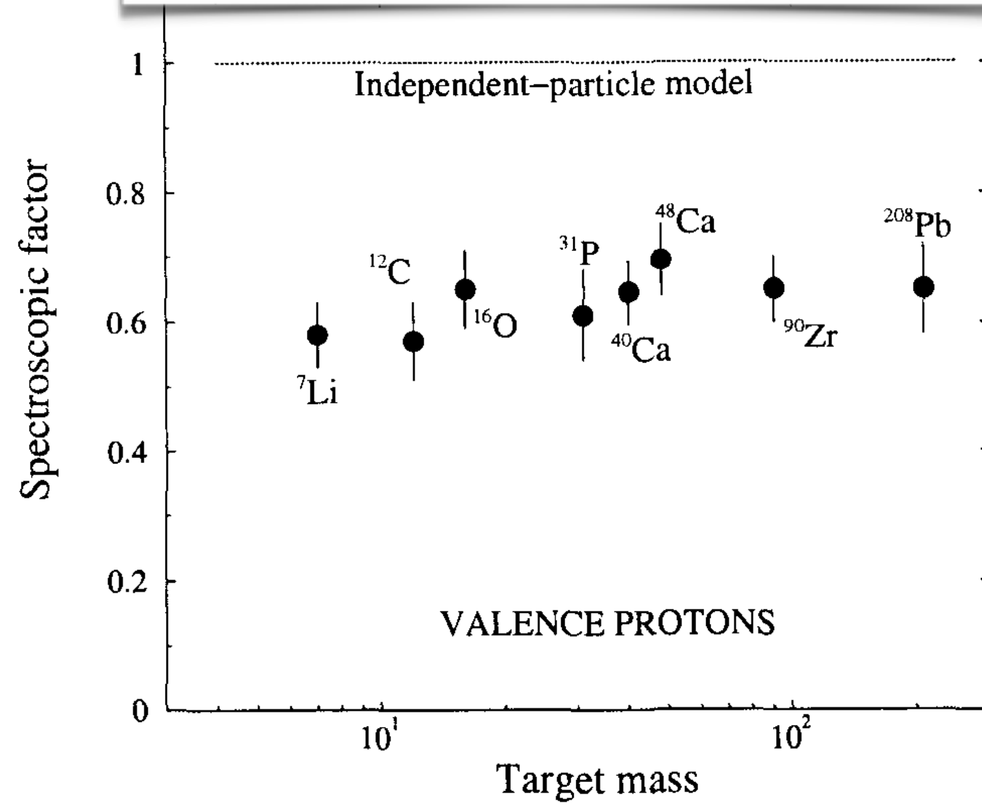

The CBF one-body Spectral Function of finite nuclei

- ^{16}O Spectral Function obtained within CBF and using the Local Density Approximation

$$P_{LDA}(\mathbf{k},E) = P_{MF}(\mathbf{k},E) + P_{corr}(\mathbf{k},E)$$

$$\int d^3r P^{NM}_{corr}(\mathbf{k},E;\rho=\rho_A(r))$$

- The one-body Spectral function of nuclear matter:

$$H = \sum_i \frac{\mathbf{p}_i^2}{2m} + \sum_{i<j} v_{ij} + \sum_{i<j<k} V_{ijk} + \dots$$

Argonne v18 (v_{ij})

UIX, IL7 (V_{ijk})

- The Correlated Basis Function approach accounts for correlations induced by the nuclear interactions

$$\Phi_n(x_1 \dots x_A) \longrightarrow \mathcal{F}\,\Phi_n(x_1 \dots x_A)$$

- The correlation operator reflects the spin-isospin dependence of the nuclear interaction

$$\mathcal{F} \equiv \left(\mathcal{S}\prod_{i<j} F_{ij}\right) \qquad F_{ij} \equiv \sum_p f^p_{ij} O^p_{ij}$$

- High energy and momentum correlated pairs

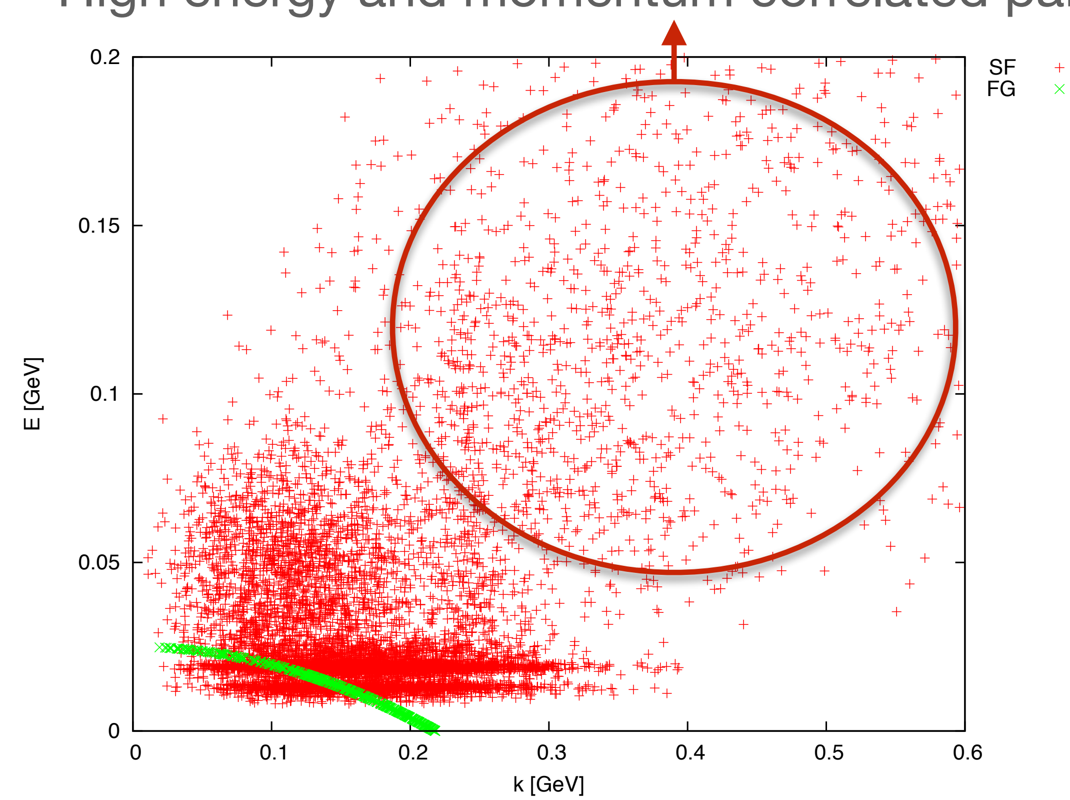

The CBF one-body Spectral Function of finite nuclei

- ^{16}O Spectral Function obtained within CBF and using the Local Density Approximation

$$P_{LDA}(\mathbf{k}, E) = P_{MF}(\mathbf{k}, E) + P_{corr}(\mathbf{k}, E)$$

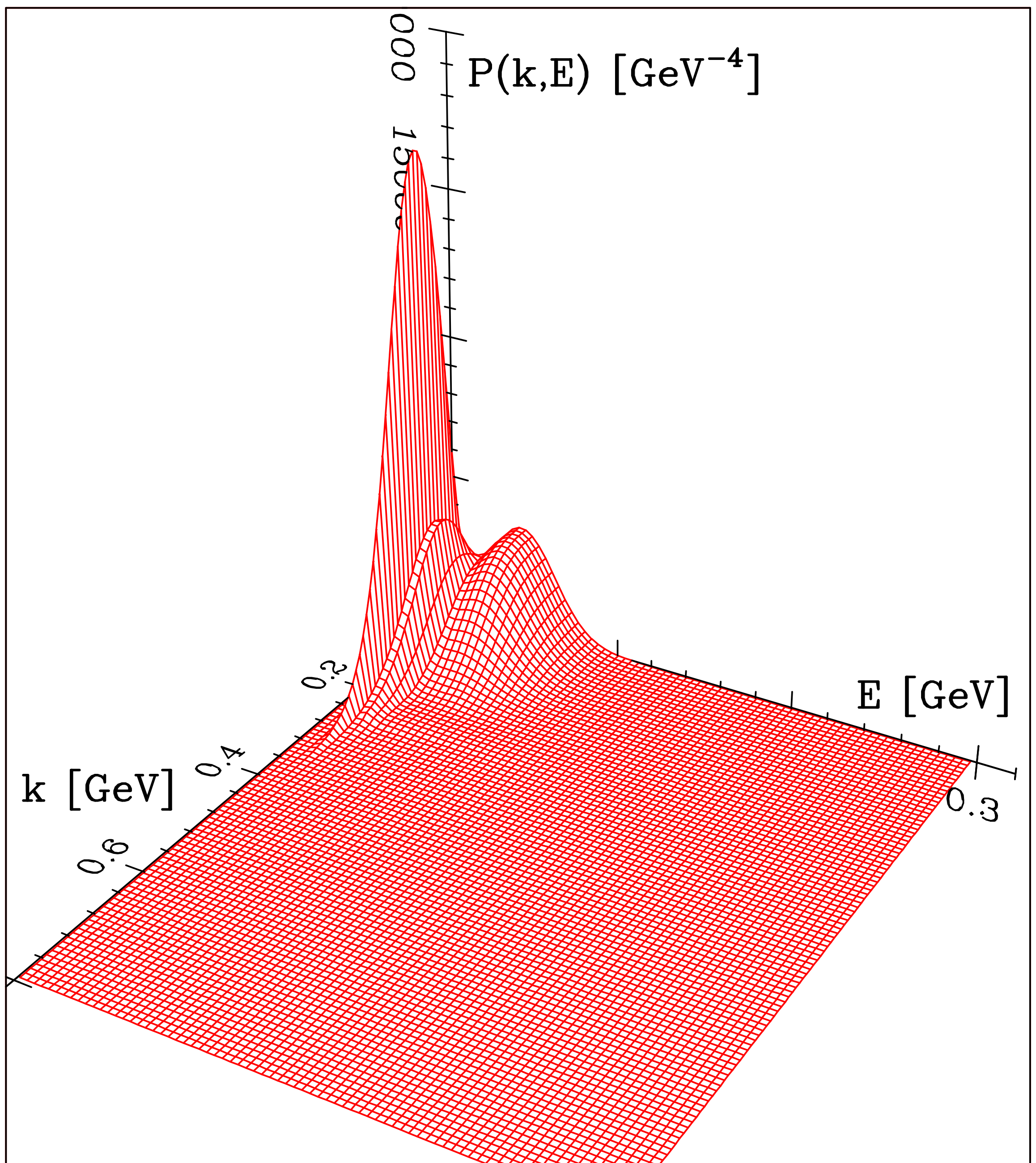

^{40}Ar: JLab E 12-14-012

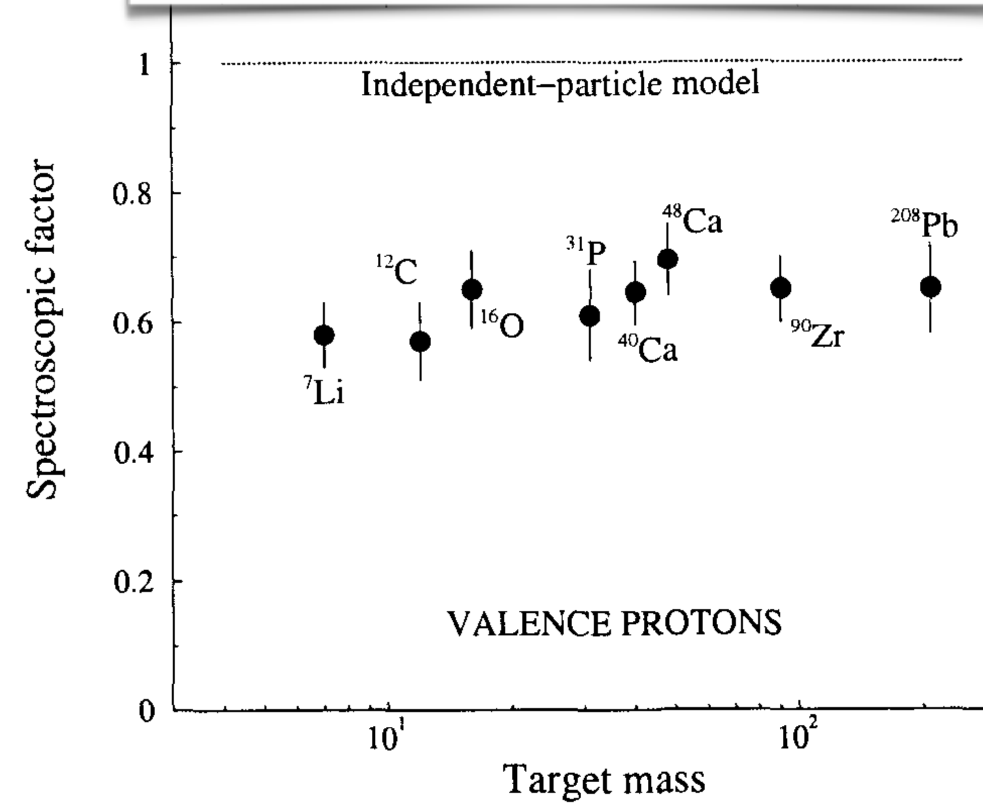

- High energy and momentum correlated pairs

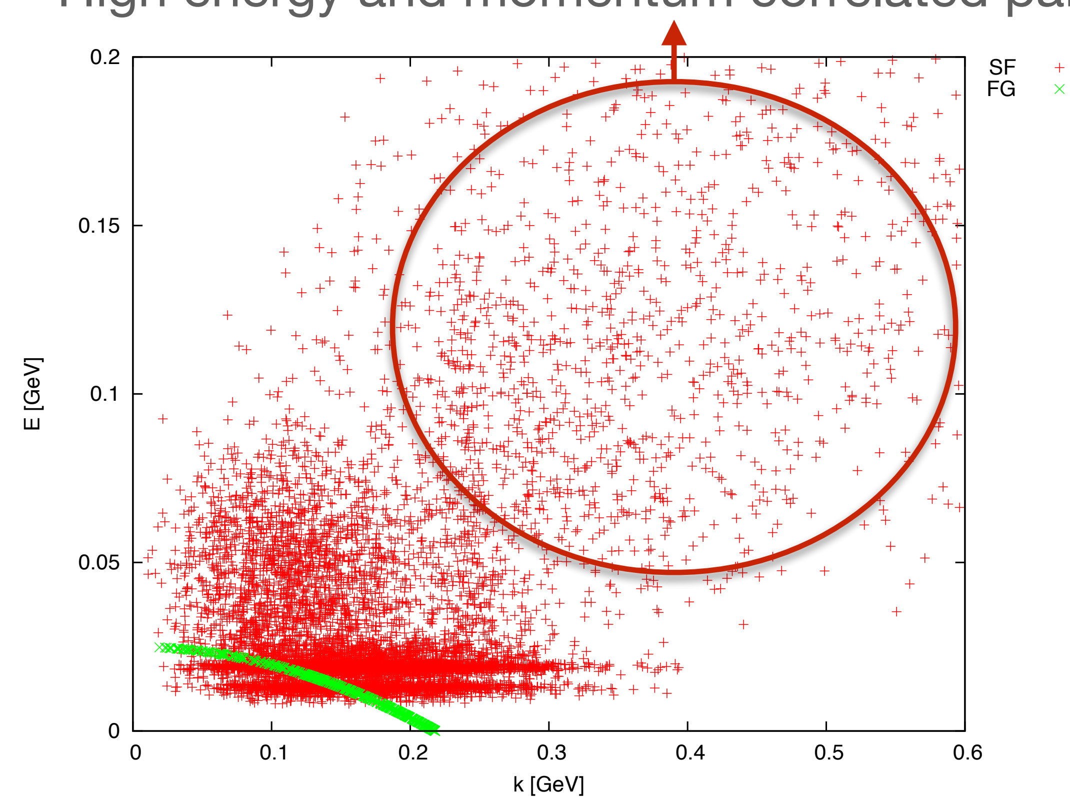

Production of two particle-two hole (2p2h) states

- Initial State Correlations

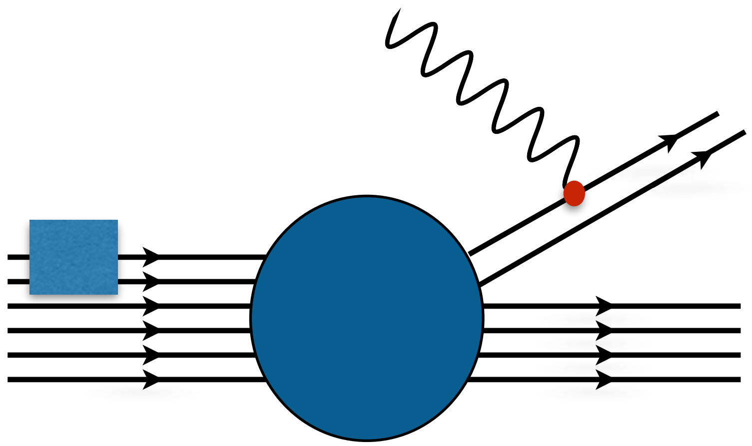

- Meson Exchange currents

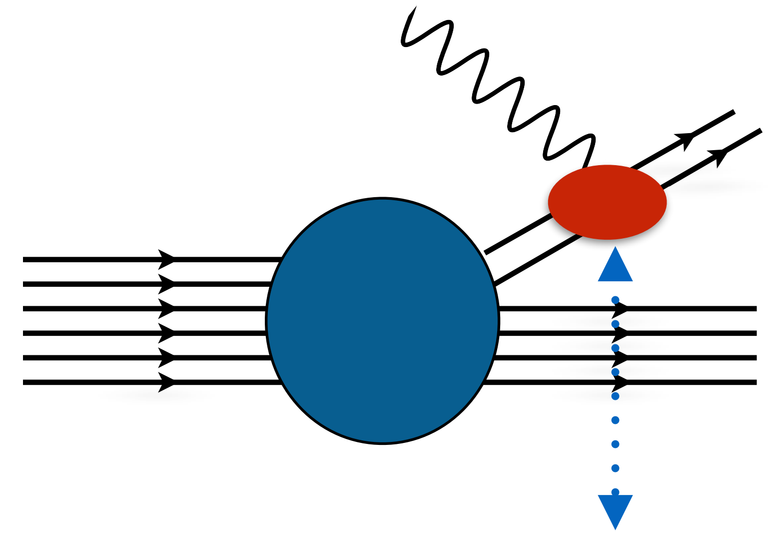

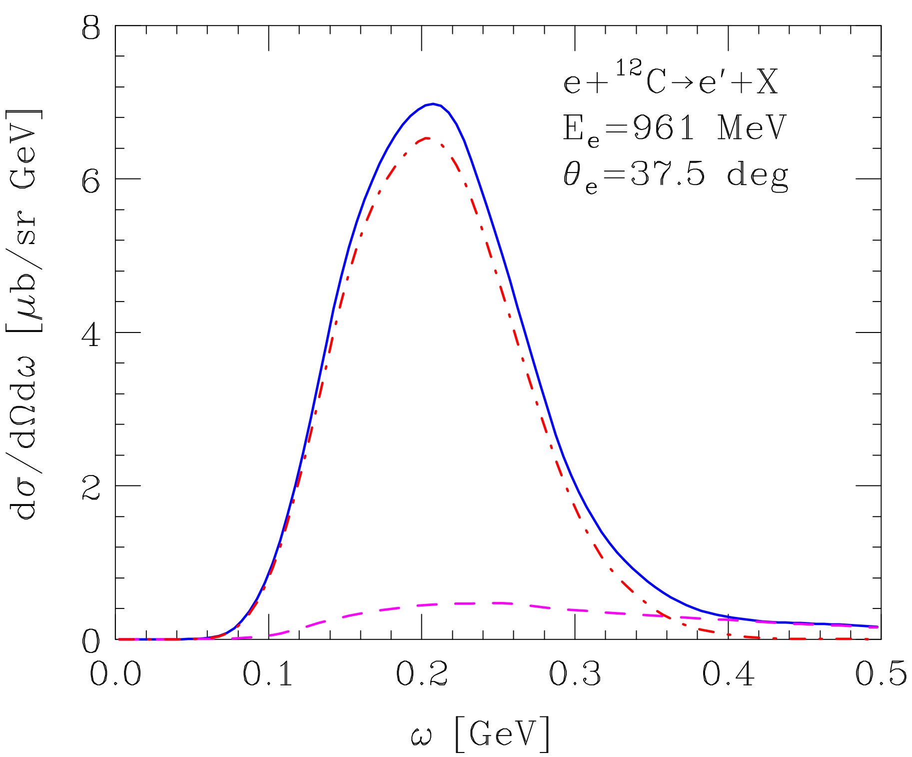

- $P_{corr}(\mathbf{k},E)$ accounts for the presence of strongly correlated pairs. Its contribution to the cross section is clearly visible: appearance of a tail in the large energy transfer region

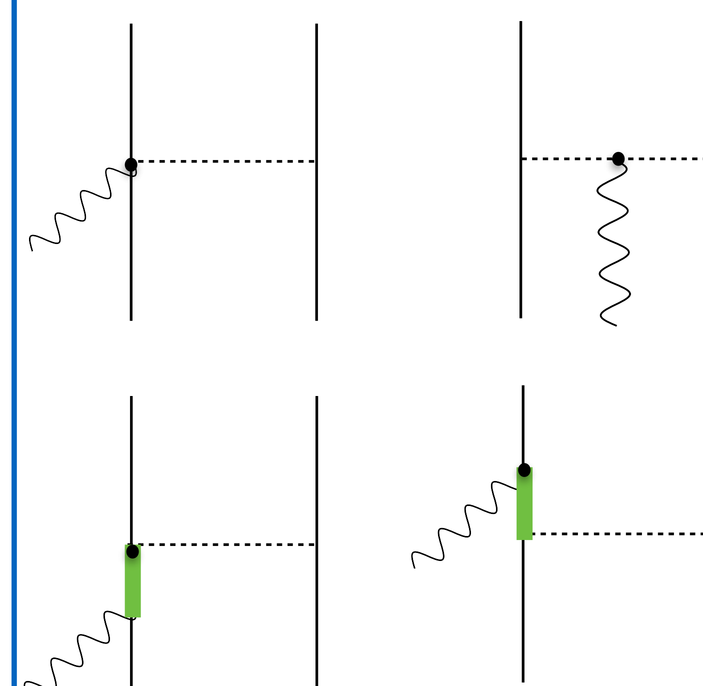

Different contributions to the relativistic two-body currents

- The Spectral Function approach has been generalized:

$$W^{\mu\nu}_{2p2h} = W^{\mu\nu}_{ISC} + W^{\mu\nu}_{MEC} + W^{\mu\nu}_{int}$$

Results for electron-^{12}C cross sections

- Separate contributions: IA

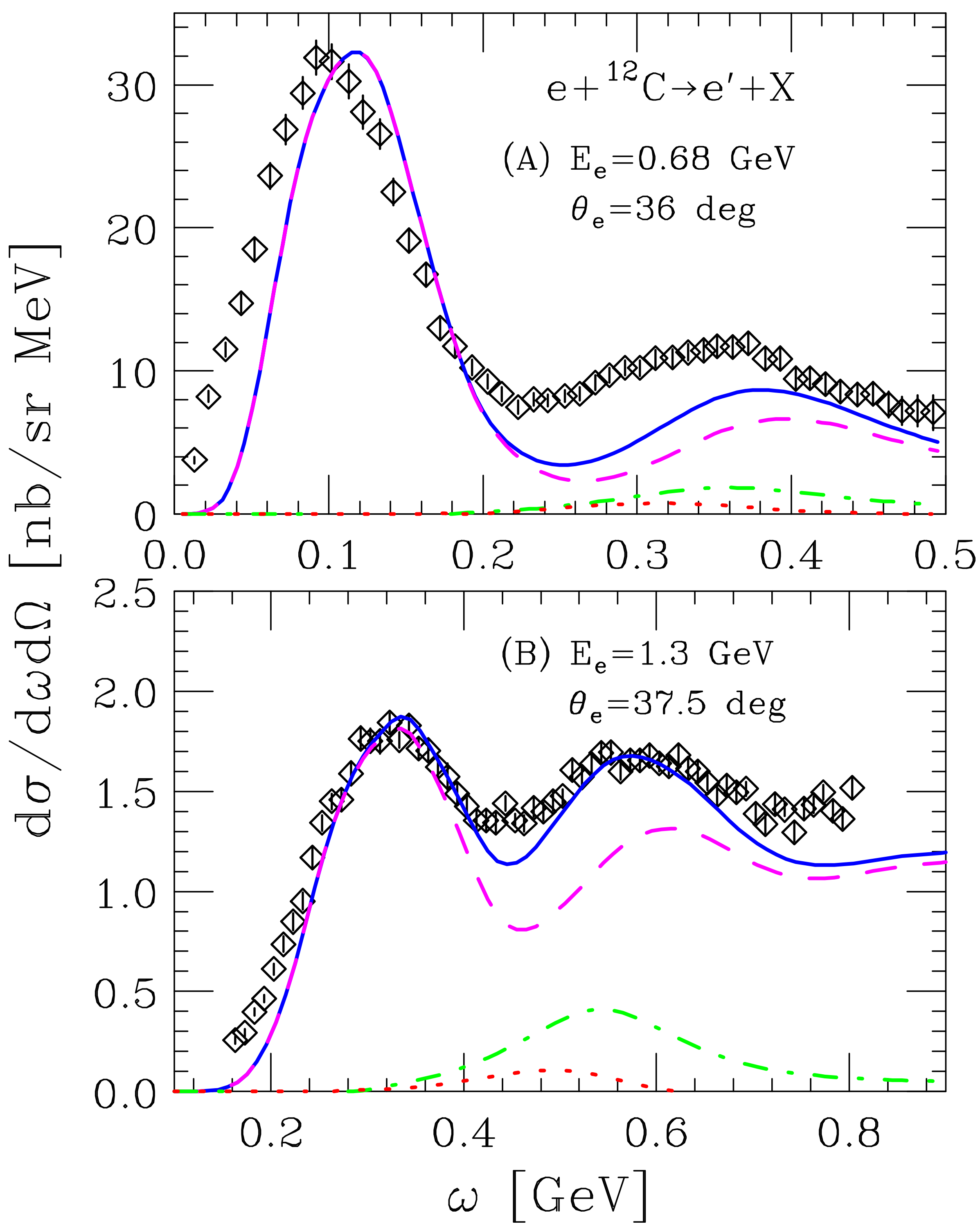

- Including FSI in the QE region

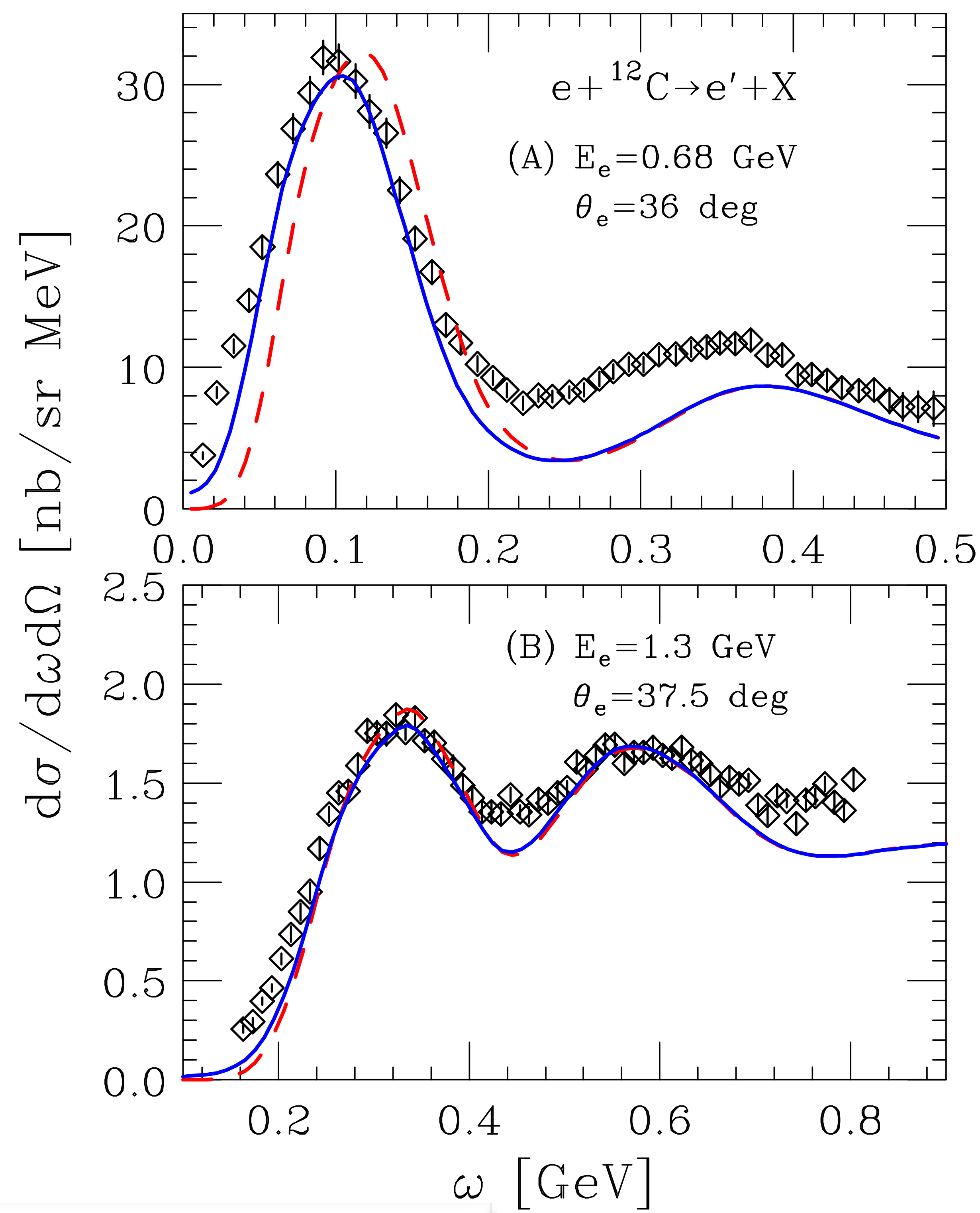

NR, A.Lovato, O.Benhar, PRL 116, 192501 (2016)

(Anti)neutrino -^{12}C scattering cross sections

The inclusive cross section of the process in which a neutrino or antineutrino scatters off a nucleus can be written in terms of five response functions

$$\frac{d\sigma}{dE_{\ell'}d\Omega_\ell} \propto [v_{00}R_{00} + v_{zz}R_{zz} - v_{0z}R_{0z} + v_{xx}R_{xx} \mp v_{xy}R_{xy}]$$

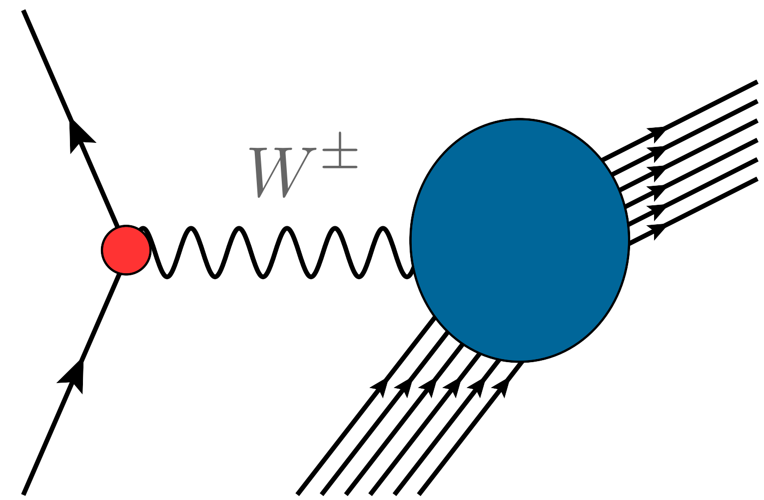

- The two-body diagrams contributing to the axial and vector responses

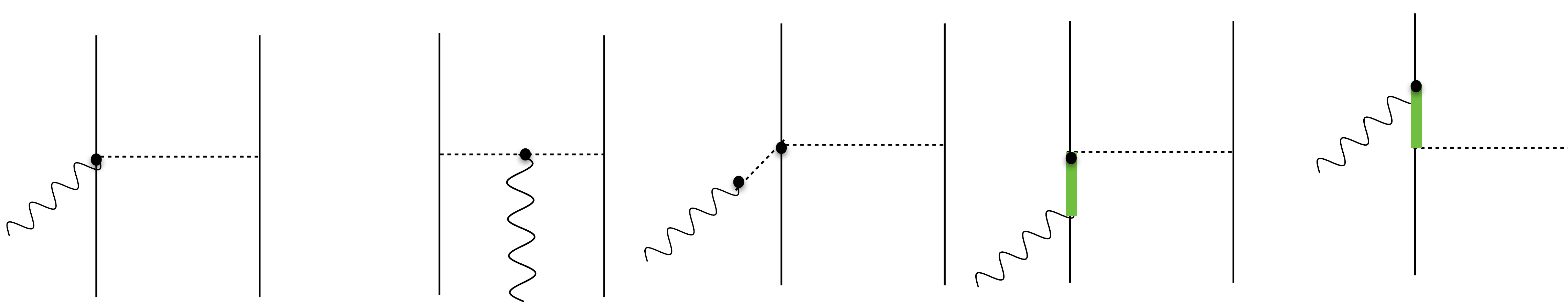

- In the preliminary results we present we only included:

$$W^{\mu\nu}_{2p2h} = W^{\mu\nu}_{ISC} + W^{\mu\nu}_{MEC} + W^{\mu\nu}_{int}$$

(Anti)neutrino -^{12}C scattering cross sections

- The exchange contribution for the 2b is still missing (antisymmetrization of the final two-nucleon state)
- The 2b contribution affects the 'dip' region, in analogy with the electromagnetic case
- Meson exchange currents strongly enhance both the neutrino and antineutrino cross section for large values of the scattering angle

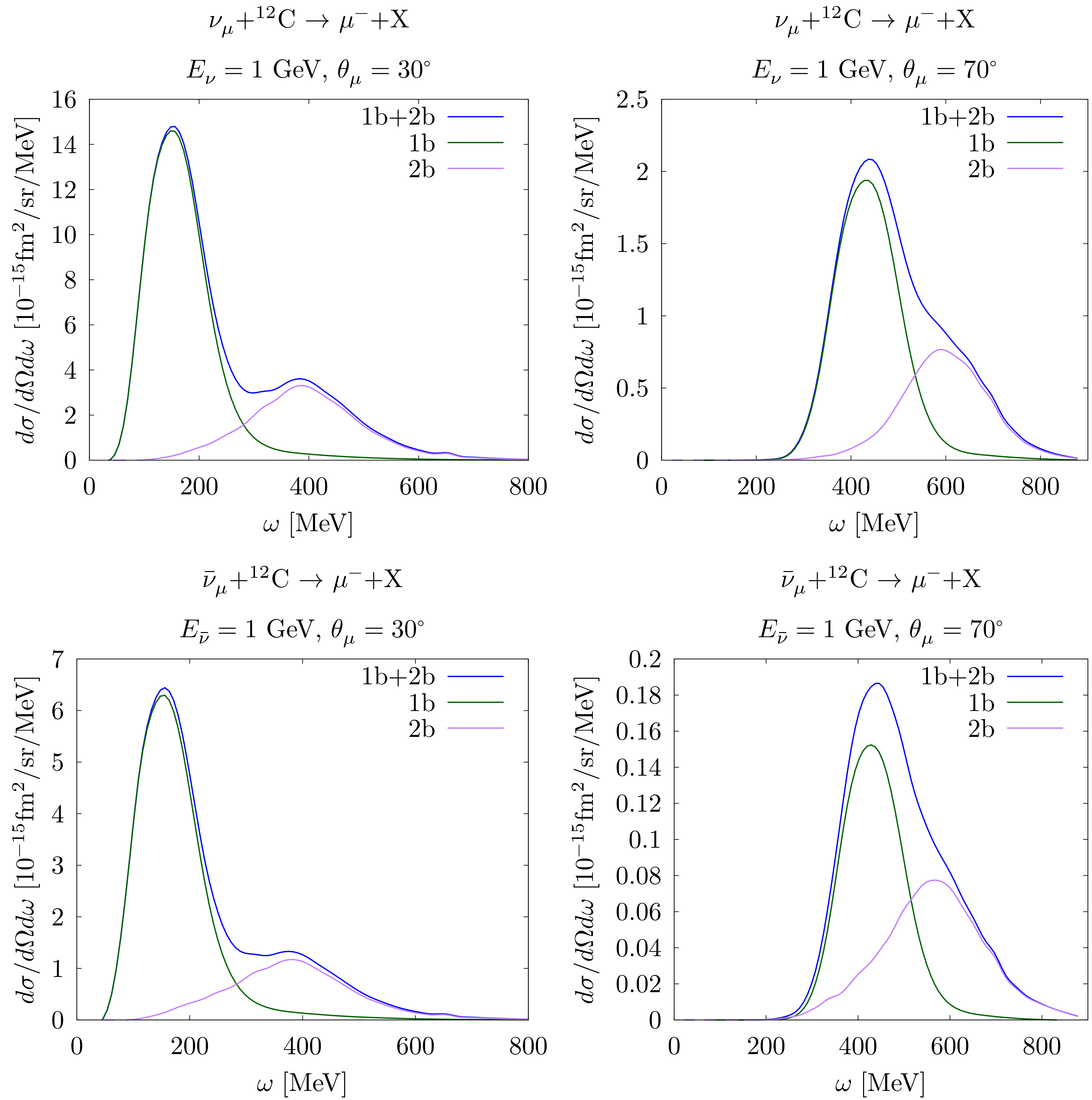

Summary and conclusions

- The Correlated Basis Function approach :
  - 😄 Accurate calculations are available for symmetric nuclear matter
  - 😄 The extension to both low- and medium-mass nuclei has been performed using the Local Density Approximation
  - 😄 Using the generalized factorization ansatz we are able do describe all the different reaction mechanisms contributing to the lepton-nucleus scattering cross sections
  - 😢 Final State Interactions are included in an approximate fashion

- The Green's Function Monte Carlo approach:
  - 😄 Accurate results for electroweak responses of ^{4}He and ^{12}C
  - 😢 The main limitations of this method comes from its nonrelativistic nature and its computational cost
  - 😄 The two- fragment model, suitable for realistic models of nuclear dynamics, has been employed to account for relativistic kinematics. Double-differential cross sections has be extracted through an accurate interpolation of the response functions.

Summary and conclusions

- The Self Consistent Green's Function approach :

😄 The Green's function calculation completely describes one-body dynamics. Modern two- and three- nucleon chiral forces can be fully exploited within this formalism

😄 We obtained the point density, charge density and single-momentum distribution of ^{4}He and ^{16}O.

😢 The center of mass contribution sizably affects these quantities for light nuclei. It cannot be separated cleanly in most ab initio post-Hartree-Fock methods.

😄 To provide an estimate of this effect in the ^{4}He results, we used a Metropolis Monte Carlo algorithm where the trial wave function we used is the Slater determinant obtained from the OpRS calculation

😄 Satisfactory results have been obtained for the electron-^{16}O double differential cross section, where the IA calculation has been supplemented by FSI

😄 The SCGF method has recently been reformulated within Gorkov's theory that allows to address open shell nuclei. Next step: extension to the electroweak sector including both one- and two-body currents.

Back up slides

Relativistic aspects of nuclear dynamics

LAB:

$$P_i^{fr} = 0$$
$$P_f^{fr} = \mathbf{q}^{fr}$$
$$p_{Nf}^{fr} = \mathbf{q}$$
$$\mathbf{q}^{fr} = \mathbf{q}$$
$$\beta = \frac{q}{M_0 + \omega}$$

- In the LAB frame, the momentum of the active nucleon is the largest

Anti-LAB:

$$P_i^{fr} = -\mathbf{q}^{ALAB}$$
$$P_f^{fr} = 0$$
$$p_{Nf}^{fr} = \frac{A-1}{A}\mathbf{q}^{ALAB}$$
$$\beta = \frac{q^{ALAB}}{M_0 + \omega}$$

- The momentum of the active nucleon is $\approx q$

Breit:

$$P_i^{fr} = -\frac{\mathbf{q}^B}{2}$$
$$P_f^{fr} = \frac{\mathbf{q}^B}{2}$$
$$p_{Nf}^{fr} = \frac{2A-1}{2A}\mathbf{q}^B$$
$$\beta = \frac{q^B}{2M_0 + \omega}$$

- The Breit frame minimizes the sum of the center of mass kinetic energies of the initial and final state

Active nucleon Breit:

$$P_i^{fr} = -\frac{A\mathbf{q}^{ANB}}{2}$$
$$P_f^{fr} = -\frac{(A-2)\mathbf{q}^{ANB}}{2}$$
$$p_{Nf}^{fr} = \frac{\mathbf{q}^{ANB}}{2}$$
$$\beta = \frac{q^{ANB}}{2M_0/A + \omega}$$

- ω^{ANB} at the QE peak is 0. This applies both to the relativistic and non relativistic case

Extension of the factorization scheme to two-nucleon emission amplitude

$$|X\rangle \longrightarrow |\mathbf{p}\ \mathbf{p}'\rangle \otimes |n_{(A-2)}\rangle = |n_{(A-2)}; \mathbf{p}\ \mathbf{p}'\rangle \ ,$$

We can introduce the two-nucleon Spectral Function...

$$P(\mathbf{k}, \mathbf{k}', E) = \sum_n |\langle n_{(A-2)}; \mathbf{k}\ \mathbf{k}'|0\rangle|^2 \delta(E + E_0 - E_n)$$

probability of removing two nucleons leaving the A-2 system with energy E

The pure 2-body & the interference contribution to the hadron tensor read

$$W^{\mu\nu}_{2p2h,22} \propto \int d^3k d^3k' d^3p d^3p' \int dE\ P_{2h}(\mathbf{k}, \mathbf{k}', E) \langle \mathbf{k}\mathbf{k}'|j^{\mu}_{12}|\mathbf{p}\mathbf{p}'\rangle\langle \mathbf{p}\mathbf{p}'|j^{\nu}_{12}|\mathbf{k}\mathbf{k}'\rangle$$

$$W^{\mu\nu}{}_{2p2h,12} \propto \int d^3k\ d^3\xi\ d^3\xi'\ d^3h\ d^3h' d^3p\ d^3p' \phi^{hh'\,*}_{\xi\xi'} \langle \mathbf{p}, \mathbf{p}'|j^{\nu}_{12}|\boldsymbol{\xi}, \boldsymbol{\xi}'\rangle$$
$$\left[\Phi^{hh'p'}_{k} \langle \mathbf{k}|j^{\mu}_{1}|\mathbf{p}\rangle + \Phi^{hh'p}_{k} \langle \mathbf{k}|j^{\mu}_{2}|\mathbf{p}'\rangle\right]$$

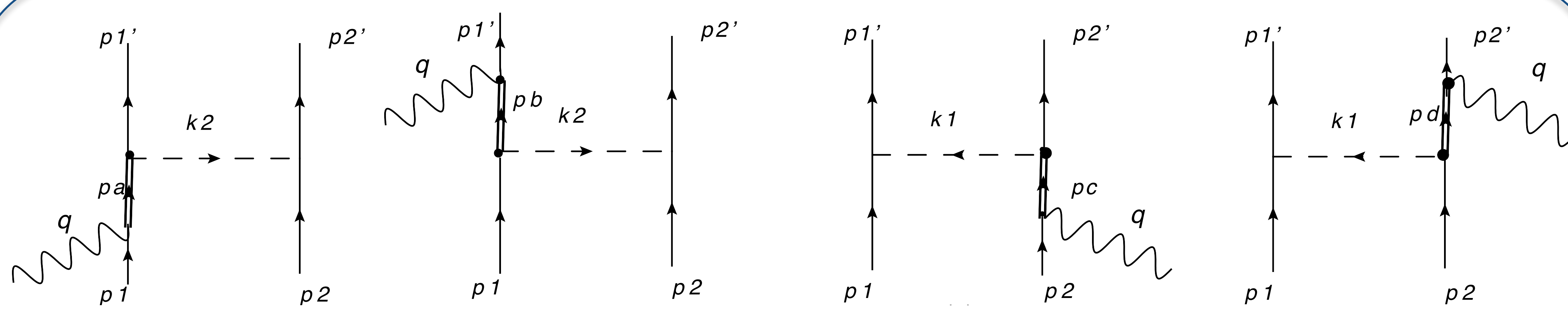

The Rarita-Schwinger (RS) expression for the Δ propagator reads

$$S^{\beta\gamma}(p, M_\Delta) = \frac{\not{p} + M_\Delta}{p^2 - M_\Delta^2}\left(g^{\beta\gamma} - \frac{\gamma^\beta\gamma^\gamma}{3} - \frac{2p^\beta p^\gamma}{3M_\Delta^2} - \frac{\gamma^\beta p^\gamma - \gamma^\gamma p^\beta}{3M_\Delta}\right)$$

WARNING

If the condition $p_\Delta^2 > (m_N + m_\pi)^2$ the real resonance mass has to be replaced by $M_\Delta \longrightarrow M_\Delta - i\Gamma(s)/2$ where $\Gamma(s) = \frac{(4f_{\pi N\Delta})^2}{12\pi m_\pi^2}\frac{k^3}{\sqrt{s}}(m_N + E_k)$.

Hadronic monopole form factors

$$F_{\pi NN}(k^2) = \frac{\Lambda_\pi^2 - m_\pi^2}{\Lambda_\pi^2 - k^2}$$

$$F_{\pi N\Delta}(k^2) = \frac{\Lambda_{\pi N\Delta}^2}{\Lambda_{\pi N\Delta}^2 - k^2}$$

and the EM ones

$$F_{\gamma NN}(q^2) = \frac{1}{(1 - q^2/\Lambda_D^2)^2} \ ,$$

$$F_{\gamma N\Delta}(q^2) = F_{\gamma NN}(q^2)\left(1 - \frac{q^2}{\Lambda_2^2}\right)^{-1/2}\left(1 - \frac{q^2}{\Lambda_3^2}\right)^{-1/2}$$

where $\Lambda_\pi = 1300$ MeV, $\Lambda_{\pi N\Delta} = 1150$ MeV, $\Lambda_D^2 = 0.71 \mathrm{GeV}^2$, $\Lambda_2 = M + M_\Delta$ and $\Lambda_3^2 = 3.5 \ \mathrm{GeV}^2$.